8-2017

# Laboratory Resistivity Measurements for Soil Characterization

Behdad Mofarraj Kouchaki
*University of Arkansas, Fayetteville*

Laboratory Resistivity Measurements for Soil Characterization

A thesis submitted in partial fulfillment
of the requirements for the degree of
Master of Science in Civil Engineering

by

Behdad Mofarraj Kouchaki
Sharif University of Technology
Bachelor of Science in Civil Engineering, 2014

August 2017
University of Arkansas

This thesis is approved for recommendation to the Graduate council.

_____
Dr. Michelle L. Bernhardt
Thesis Director

_____
Dr. Clint M. Wood
Committee member

_____
Dr. Gary S. Prinz
Committee Member

**Abstract**

Field based electrical resistivity measurements, such as electrical resistivity tomography (ERT) and capacitively coupled resistivity (CCR), are geophysical methods that offer a non-destructive and rapid means to collect continuous data. As such, ERT and CCR are becoming increasingly popular tools for geotechnical engineers; however, it is challenging to derive geotechnical information such as soil type, density, and water content from the data. A laboratory geophysical investigation was carried out to gain a better understanding of the parameters that affect the electrical resistivity of soils and devise a relationship between resistivity and soil type or classification. In this study, a soil box attached to a resistance meter in a 4-electrode Wenner array was used for the resistivity measurements. Nine different benchmark soils were tested, representing most of the major soil groups according to the unified soil classification system. The effects of water quality, water content, degree of saturation, bulk density, dry density, Atterberg limits and temperature on the measured electrical resistivity of the soils were investigated. Although there is an apparent correlation between all of these parameters and the electrical resistivity of soils, the parameters that are most effective in the identification of soil type are bulk density and degree of saturation. The laboratory results indicate that if the soil is saturated, a reasonable estimate of the soil group classification can likely be made from resistivity alone. For unsaturated samples, the range of possible resistivity values is much larger; however, the estimate of soil group can be significantly narrowed down if an approximation of saturation or density can be made. To assess the feasibility of the developed approach, a series of verification studies using samples acquired from the field and other processed soils were also conducted.

**Acknowledgments**

First and foremost, I am thankful to god for all the blessed relationships I have formed during my Master's studies in school and in society which allowed me to give back and contribute to our society through this research.

I would like to thank Dr. Bernhardt, my advisor, for accepting me as her student and giving me the opportunity to study at the University of Arkansas. This research would not have been possible without her thoughtful advising and words of encouragement. I would also like to thank Dr. Wood for his guidance throughout this research project. Moreover, I would like to thank my colleagues, Mr. Moody and Mr. Deschenes who collaborated in this project as well; we shared many laughs in the field.

I would also like to thank Dr. Prinz as a member of my thesis committee for taking the time to evaluate this thesis and providing valuable feedback.

Most importantly, I would like to thank my wonderful parents who gave me courage to study in another country and bore the burdens of this long distance relationship. None of this would have happened without their sacrifices and the support they provided me when life became overwhelming.

There are many other individuals to thank, without whom I would not have been where I am standing now; Ms. Pournoman, Mr. & Mrs. Stilwell and Mr. Grove, Dr. White and last but not least my wonderful friends in International Culture Team who gave a new meaning to my life.

**Dedication**

I dedicate this thesis to my wonderful family in Iran and the States for helping me become who I am today and supporting me throughout this program.

**Table of Contents**

## Chapter 1: Introduction

### 1.1 Motivation for this Study

According to the Federal Emergency Management Agency (FEMA) a levee is a "man-made structure, usually an earthen embankment, designed and constructed in accordance with sound engineering practices to contain, control, or divert the flow of water so as to provide protection from temporary flooding" (FEMA, 2006). For the levees to perform their intended function, they must be constructed of strong, compacted layers of soil that create an impervious barrier that can resist the forces of the floodwaters. Levees not only have to prevent water from seeping through the core and foundation, it is also important that the water does not erode away the soil. To create this high strength, low permeability structure, levees are ideally built in layers of compacted soil starting at the ground surface and continuing until the desired height is reached (Figure 1).

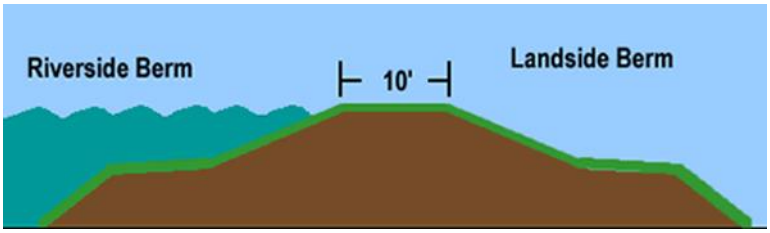


Figure 1 – Cross-section of a typical levee showing flat crest and riverside and landside slopes [Online image] Retrieved May 1, 2017 from: http://library.water-resources.us/docs/MMDL/FLD/Feature.cfm?ID=5

In 2017, the American Society of Civil Engineers (ASCE) gave the levee system in the United States an overall rating of D (ASCE, 2017). This report indicates there is currently 48,000 documented kilometers (30,000 miles) of levees in the U.S. surrounding communities, critical infrastructure, and property with an estimated value over $1.3 trillion. According to this report, most of the levees in the U.S. were built in the middle of the past century by federal, state, and

local agencies or by private property owners and are 50 years old on average. Although many levees were originally made to protect farmland, due to urban sprawl and changes in land use, over 14 million people now live or work behind these structures.

Although numerous flood related failures have occurred throughout history, prior to 2005, most of these failures were in low-risk rural areas where damages were mostly agricultural related. The first real failure to occur in an urban environment came in August of 2005 during Hurricane Katrina. The levees and floodwalls in and around New Orleans, Louisiana failed in over 50 locations, flooding more than 80% of the city, killing over 1,118 people, and resulting in an estimated $16.5 billion in damages (ASCE, 2007). Considered the most costly US natural disaster on record, these events exposed the vulnerability and increased risk associated with levee systems surrounding growing urban developments. In 2007, Congress directed agencies to create a national levee database and in 2009, ASCE created a new category for levees in its report card for America's infrastructure. Levees received a grade of D-, which was a less than poor rating, but it increased awareness of the issue, the limited funds available, and provided a general plan to address the deteriorating system. Two additional major flood related disasters occurred in the Midwest in 2008 ($538 million in estimated damages) and in 2011, where record water levels resulted in over $2 billion in damages and repairs (ASCE, 2013). In the 2013 report card for America's infrastructure, the American Society of Civil Engineers gave the levee system in the United States the same overall rating of D-, showing no change from the previous report. Although levee failures in the United States account for more economic impact than any other geo-related disasters, little improvement has been made to the overall levee system. This could prove to be a major problem in the coming decades, where continued deterioration, urban

development, and an increase in extreme weather events will test these structures to and beyond their capacity and significantly increasing the risk associated with their failure.

To date, the U.S. Army Corps of Engineers (USACE) has performed risk assessments on over 1,200 levee systems out of the 2,500 in their program. The assessment criteria included possible loading events such as floods, storms, and earthquakes, level of performance and consequences of failure. Major deficiencies include culverts, seepage and vegetation. The risk-assessment results showed that 5% are at high to very high risk, 15% at moderate risk, and 80% at low risk; the numbers of high and moderate risk levees are expected to grow as more inspections are performed and awareness of their conditions is increased. Although USACE and FEMA are working to inventory levees in the US, limited funding is available to assess the condition of the levees. Without the condition and performance evaluation of a particular levee, there is no way to determine the risk associated with it.

Typically, levees are evaluated based on a simple visual inspection program to identify critical or weak spots in the system (USACE 2014). This method can detect surface distress or erosion failures (post failure), but it cannot identify defects that exist within the inner core or foundation soil that could lead to a failure during an extreme event. This leads to a passive detection system in which failures must occur often times before they are investigated. The methods currently used to proactively obtain this internal soil data are extremely time intensive, they require soil borings or sampling which damages the levees, and they only provide a small discrete amount of data. With the limited funds available, it would be impossible to obtain the data needed to properly evaluate the condition of the nation's levees using these invasive methods. Therefore, there is a need for a rapid, proactive, non-destructive assessment procedure

that can quickly and cost effectively gather continuous data, so that the most accurate performance evaluation can be made before defects in the levee lead to catastrophic failures.

### 1.2 Organization of Thesis

As discussed, many of the defects leading to levee failure are internal problems that depend on the materials used in levee construction. However, due to the limited funding available and the vast number of levees, inspections rarely go beyond visual inspection which cannot identify such problems before it is too late. Therefore, there is great need to determine the most cost-effective non-destructive testing methods which can be used to quickly and reliably identify the subsurface soils and any deficiencies. The main objective of the research presented in this thesis is to develop an approach, based on electrical resistivity testing, to rapidly and non-destructively assess levee subsurface soils. Using this and other geophysical methods, the ultimate goal is that someday the overall condition of the levees, including the most critical locations in need of repair will be able to be determined through a quick and cost-effective assessment.

Following this introduction, Chapter 2: Background presents background information related to levee failures and possible non-destructive technologies which may prove useful for future more robust levee inspections and assessments. A discussion of the rationale behind the chosen method is also provided. Chapter 3: Research methodology presents the methodology including the laboratory setup, procedures, and details of any special considerations made. Following the methodology, the goal of the research was to identify the effect of various engineering parameters such as density, water content, saturation, temperature and water quality on the electrical resistivity of soils in order to link electrical resistivity measurements with soil

type. A series of controlled laboratory experiments were carried out using a Nilsson Resistance Meter Model 400 attached to a M.C. Miller Large Soil Box in a Wenner 4-electrode array. In these tests, numerous resistivity measurements were taken using different soil types under controlled laboratory conditions to understand the link between this geophysical testing method and the engineering properties of interest. Chapter 4 presents the results of the study and Chapter 5 contains the conclusions and final remarks.

## Chapter 2: Background

### 2.1 Levee Defects and Failure Mechanisms

Many mechanisms could lead to a levee's failure. Some of the most common failure mechanisms are shown in Figure 2. These failure mechanisms are often divided into two categories: structural failures and failures due to hydraulic forces. Structural failures include damage to the embankment from debris or tree uprooting, slope failures, and sliding, while failures from hydraulic forces include underseepage, overtopping or wave erosion, piping, and liquefaction.

The following sections summarize the most common levee failure modes and the defects that lead to these failures (Ellis et al. 2008 and Vrjiling 2003). It should be noted that although these are termed failure modes, their occurrence does not guarantee catastrophic failure of the levee. Breaching is often caused by a combination of these failure modes.

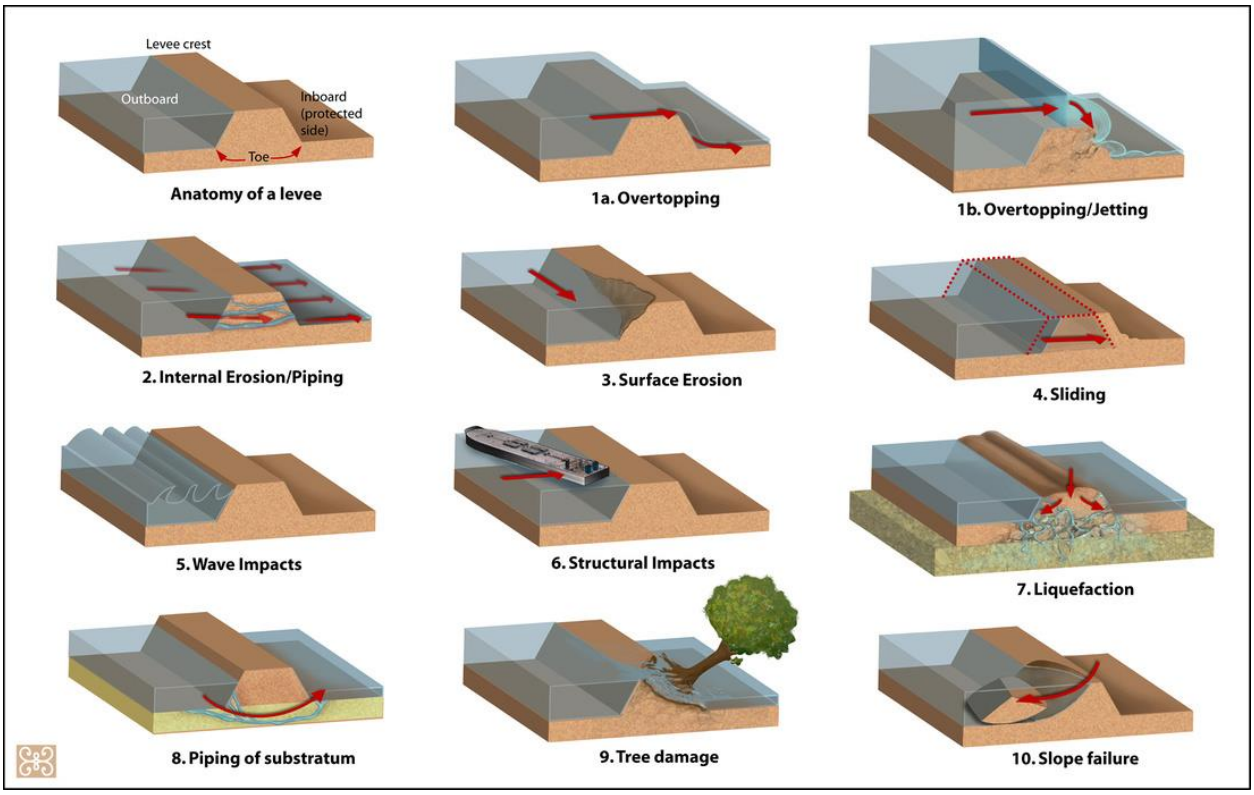


Figure 2 – Deretsky, Z. (2010) Ten ways a levee can fail. [Online image], retrieved on July 18, 2017 from http://www.zina-studio.com/p489212137/h1834C228#h1834c228

### 2.1.1 Overtopping Erosion

One of the most common phenomenon causing levee failures is surface erosion due to overtopping (Figure 3). In this process, the dry side of the levee will start being eroded by the forces of the overtopping water which may result in steepening of the downstream slope, lowering of crest, head cut development, and eventual collapse of the structure. There are many factors which affect the rate of erosion including grain size distribution, compaction energy, salinity of water, levee geometry and vegetative cover. As indicated by Briaud et al. (2008), larger grained soils such as sands are more susceptible to erosion compared to fine grained soils such as clays. The slope of the levee, determines the velocity of the water jet on the dry side where higher velocity corresponds with a higher rate of erosion. Generally, plants with extensive

root networks help protect the soil from eroding by keeping the soil particles in place and decreasing the speed of water flow (Figure 4). There are number of ways to mitigate this erosion process including adequate design to prevent overtopping, providing vegetation cover, avoiding erodible soils and steep slopes. Visual inspection of the levee is sufficient in assessing the susceptibility to overtopping erosion and there is no need for additional assessment tools. The two items which should be checked are a comparison of the current height of the levee with the design height, and the vegetative coverage.  As shown in Figure 4, good vegetative cover can help armor the levee from surface erosion.

Figure 3 - overtopping erosion in a levee west of Oakford, IL (Rutherford et al., 2016)

Figure 4 - vegetative cover laid down and acting as an armor on the landside slope of the levee near Olive Branch, IL (Rutherford et al., 2016)

### 2.1.2 Internal erosion/ Piping

Another common failure mechanism associated with levees is failure due to internal erosion or piping. In this phenomenon, a series of pipes or water paths will develop in the body of the levee, due to the existing hydraulic gradient, enabling the transportation of water from the wet side to the dry side of the levee. In this process water goes through the path which satisfies the criteria for relatively higher hydraulic conductivity and higher hydraulic gradient. Through time, water carries smaller soil particles with itself causing cavities to form in the levee. These cavities start forming on the dry side of the levee and propagate towards the wet side through time. Therefore, as time passes, these cavities expand and weaken the levee's core, making it more susceptible to collapse.

There are several visual signs which may indicate the occurrence of this phenomenon including the appearance of sand boils on the dry side of the levee (Figure 5), levee toe erosion, cracks on levee surface, absence of fine grain overburden materials on the dry side. The piping can also be initiated by the presence of voids from tree roots or animal burrows (Figure 6). While all levees are susceptible to piping, relatively thin levees, presence of high hydraulic gradients, and levees built with erodible soils are more susceptible to piping.

This internal erosion may occur in the foundation as well. In this case, the foundation material is much more permeable than the body material which provides a higher hydraulic gradient for water to flow through. As a result, fine-grained particles would be washed with water and transported upstream, slowly forming the void spaces in the levee foundation. This could especially happen if the levee is founded on paleo channels which comprises highly permeable and erodible sedimentary deposits. While generally the sand boils appear close to the toe, (Figure 7), visual detection of this mechanism may be harder as the sand boils may be found hundreds of meters away from the levee (Figure 8).

While burrows or sand boils can often be seen at the surface through visual inspection, internal piping or voids may not be visible and thus, a detection method capable of penetrating through the levee is needed to assess susceptibility of a levee to internal erosion. Additionally, a thorough assessment of the core and foundation soil types could also help identify soils which might be susceptible to internal erosion.

Figure 5 - The arrow indicates the location of a sand boil near the landside levee toe and the box indicates subsidence in levee crest due to loss of soil (Rutherford et al., 2016)

Figure 6 – View looking at exposed western edge of breach in a levee revealing the presence of animal burrows within the levee (Rutherford et al., 2016)

Figure 7 - Large sand boil network at levee toe near Olive Branch, IL (Rutherford et al., 2016)

Figure 8 - Sand boils approximately 1,200 feet landward of the levee with water still seeping through near Cairo, IL (Rutherford et al., 2016)

### 2.1.3 Surface erosion (Wet side)

Another common failure mechanism for levees is the erosion of soil on the water or wet side of the levees. Similar to the erosion of the land or dry side, soils on the wet side can be eroded due to the forces of flowing water. Providing adequate vegetative cover, proper compaction and avoiding erodible soils are the main solutions to avoid this type of failure. One of the most comprehensive works on erodibility of different soil types is presented in Briaud (2008) where soils are categorized into six groups depending on their erodibility from very high erodibility to non-erosive (Figure 9). As can be seen, as the plasticity of the soil increases and/or the grain size decreases, soils can resist higher shear stresses and will erode at a slower rate. Therefore, depending on the expected water velocity, suitable levee construction material must be chosen.

Visual inspection may be helpful in detecting areas where surface erosion has started developing. However, many times the water may cover the erosion issues and it would be more advantageous to use non-destructive tools to assess the erodibility of soils and be able to make an assessment of the probability of erosion occurring for a given event.

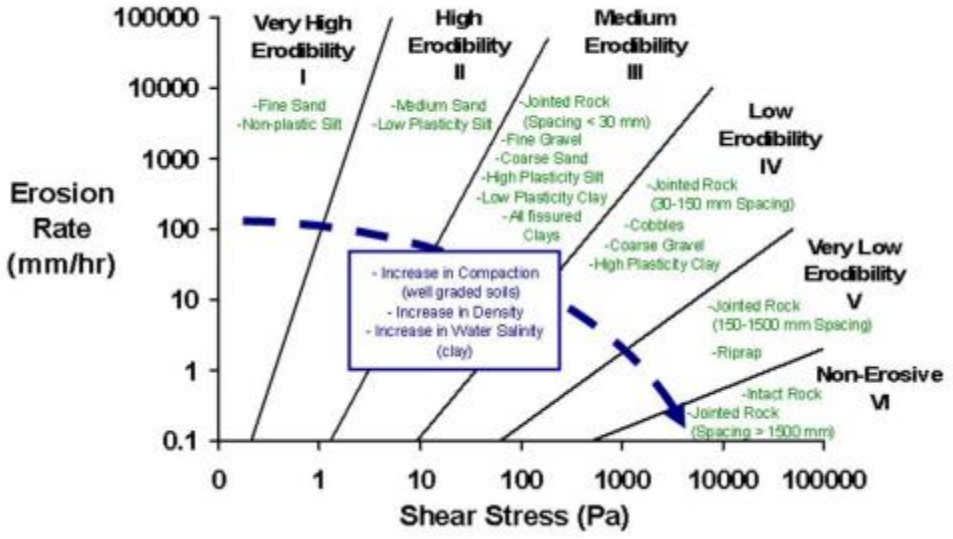


Figure 9 - Proposed erosion categories for soils and rocks based on shear stress (Briaud, 2008)

### 2.1.4 Sliding

Another failure mechanism threatening the stability of levees is failure due to sliding. In this process, the horizontal hydraulic pressure overcomes the shearing resistance provided at the interface of the levee's body and foundation and causes the levee to slide. This type of failure is likely to occur in levees where there is a sudden change of soil properties between the body and foundation materials. Although not very common, this phenomenon could occur for relatively tall levees where the levee's body is not connected adequately to the foundation. This type of failure can be prevented by increasing the bottom width of the levee and proper compaction of the bottom layer of the levee where it joins with the levee foundation.

As the sliding plane is unavailable for visual inspection, non-destructive test methods can be used to detect sharp contrast between the body and foundation materials. For example, sharp contrast between soil layers can be detected by an array of geophysical methods including seismic methods which are based on reflection and refraction.

### 2.1.5 Wave/Structural impacts

Wave impact is another process during which the levee structure will slowly deteriorate over time. Similar to other surface erosion processes, choosing the right soil and providing adequate vegetation could slow this process significantly.

Structural impacts are another cause of levee failures which may be due to the impact of boats or tree logs and other debris carried by the river during the flood. Such impacts may expose the core of the levee to the passing water and expedite the erosion. Any defects due to structural or wave impacts would be clear through visual inspection and no additional methods of detection are needed.

### 2.1.6 Liquefaction

Although there are not many documented cases for liquefaction in levees, it is another possible failure mechanism threatening levees. Generally, levees built using liquefiable soil or founded on liquefiable soil close to active faults are susceptible to liquefaction. One of the most interesting cases regarding levee liquefaction occurred in 1993 Kushiro-oki earthquake in northern Japan (Sasaki et al., 1995). The Kushiro river levees were underlain by a non-liquefiable peat layer. However, this highly compressible layer had subsided in a concave shape, creating a saturated zone in the levee as shown in Figure 10. Although liquefaction is a complex phenomenon, saturated sand layers subject to shaking have high liquefaction potential. To assess the liquefaction potential of a site, information about the potential seismic activity of the site and subsurface conditions are needed which cannot be obtained through visual inspection. However, non-destructive methods, such as Multi-Channel Analysis of Surface Waves (MASW) can confidently estimate the stiffness of subsurface layers which can be used to estimate liquefaction

potential. Resistivity methods are also capable of distinguishing between sands and other fine-grained soils.

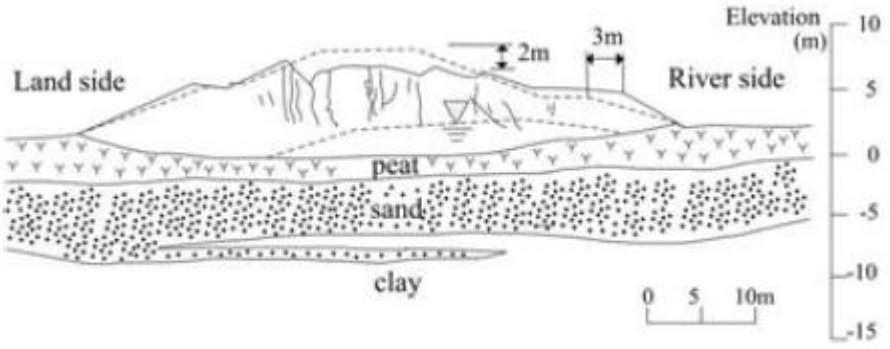


Figure 10 - Damaged levee of the Kushiro river (Sasaki et al., 1995)

### 2.1.7 Tree damage

Another potential threat to levee stability is the growth of larger plants such as trees on the levees. While under a normal climate trees may not damage the levee, severe climates such as storms could exert extreme forces on the tree and levee. If the tree gets uprooted, it will expose the levee's core and expedite the erosion process. Therefore, while grass vegetation is desired, it is often good practice to prevent trees from growing on top of the levees. Visual inspection methods would be adequate for detecting trees on levees, although it is difficult to identify the full extent of the root structure by this method.

### 2.1.8 Slope failure

Slope failure on the levee face can occur on the landside or waterside of the levee and reduce the thickness and/or height of the levee, ultimately reducing the stability. Slope failures can be the result of scour or overtopping erosion, seepage, desiccation cracking, rapid

drawdown, earthquake loading, impacts, or simply low strength soil combined with the geometry of the levee slope. Scour and seepage are typically soil type dependent.

Factors such as insufficient compaction, desiccation cracking and rapid drawdown could increase the chances of slope failure. An example surface slide due to 2016 Midwest floods is shown in Figure 11. The exposed surface was immediately covered with plastic liner and sand bags to prevent further erosion until reconstruction finished.

In this case, non-destructive testing methods and visual methods are both required to examine the subsurface soil structure and the geometry of the slope in order to assess the risk of slope failure in levees.

Figure 11 -Surface slide covered with plastic liner and sandbags near Grand Tower, IL (Rutherford et al., 2016)

## 2.2 Detection and Evaluation Methods

There are currently numerous destructive and non-destructive methods available to detect anomalies and weak points within the ground. Although the data obtained through destructive methods is generally reliable and easier to use for geotechnical engineering purposes, it demands more time and money to obtain; these methods are also undesirable for levees in particular due to their destructive nature. As discussed, a large portion of the nation's levee system has little or no data regarding the current condition or design and the data that does exist is minimal in its consideration of subsurface defects. Therefore, it is critical to develop a low-cost, rapid and non-destructive testing framework to assess the condition of the aging levee systems and repair or reinforce these structures against future floods.

### 2.2.1 Non-destructive Assessment Methods

Non-destructive geophysical tests use electrical currents, electromagnetics and stress waves to "see" within the earth without drilling or punching holes. The tests are typically conducted from the ground surface and are used to image objects or soil layers to determine the engineering or geologic properties of the subsurface. Geophysical methods that can and have been applied to levee evaluation include the Multi-channel Analysis of Surface Waves (MASW), P- and S-wave refraction, Ground Penetrating Radar (GPR), electromagnetics (EM), and capacitively coupled resistivity (CCR) (Hayashi and Konishi 2010, Lane et al. 2008, Inazaki and Sakamoto 2011, Kita et al. 2013, Mckenna et al. 2006). Each of these methods has distinct features that make them advantageous for detecting various defects within a levee system. For example, MASW and S-wave refraction provide a shear wave velocity (Vs) profile of the levee that is directly related to the shear modulus of the levee. This profile can be used to detect low

density areas and strength related to weak spots within the levee and foundation system that could lead to failure. In addition, the Vs profile can be used to evaluate the liquefaction potential of various levee and foundation layers. The P-wave refraction method can determine the P-wave velocity profile of the levee and most importantly, it can be used to identify the line of saturation through the levee for liquefaction analysis and seepage monitoring. GPR can detect small buried objects, pipes, and other encroachments within the levee which can create weak spots and piping/seepage zones within the levee. EM and resistivity measurements can be used to infer the soil type of the levee and pick up changes in soil type with depth. Some of the most common geophysical methods will be described in more detail in the following subsections.

#### 2.2.1.1 Electromagnetic surveys (EM)

Electromagnetic induction is a method to measure the apparent electrical conductivity of subsurface materials. Electrical conductivity is a measure of how well the soil conducts an electrical current. These measurements can be used to identify geologic materials and their locations. It can also be used for identifying buried metallic items. Conductivity values vary over several orders of magnitude depending on the type of material (Table 1). It is known that the amount of pore fluid present, the salinity of the pore fluid, the presence of conductive materials, and the amount of fracturing influence the conductivity measurements. (Llopis and Simms, 2007)

Table 1 – conductivity and electrical resistivity values of some common rocks and minerals (Keller and Frischknecht, 1966)

| Material | Resistivity, Ω-m | Conductivity, milliSiemens/m (mS/m) |
|---|---|---|
| **Igneous and Metamorphic Rocks** | | |
| Granite | $5\times10^3$ – $10^6$ | 0.001 – 0.2 |
| Basalt | $10^3$ – $10^6$ | 0.001 – 1 |
| Slate | $6\times10^2$ – $4\times10^7$ | $2.5\times10^{-5}$ – 1.7 |
| Marble | $10^2$ – $2.5\times10^8$ | $4\times10^{-6}$ – 10 |
| Quartzite | $10^2$ – $2\times10^8$ | $5\times10^{-6}$ – 10 |
| **Sedimentary Rocks** | | |
| Sandstone | 8 – $4\times10^3$ | 0.25 – 125 |
| Shale | 20 – $2\times10^3$ | 0.5 – 50 |
| Limestone | 50 – $4\times10^2$ | 2.5 - 20 |
| **Soils and Waters** | | |
| Clay | 1 – 1000 | 1 – 1000 |
| Alluvium | 10 – 800 | 1.25 – 100 |
| Groundwater (fresh) | 10 – 100 | 10 – 100 |
| Sea water | 0.2 | 5000 |

For measurement of soil conductivity through EM induction, a transmitter (Tx) and a receiver (Rx) coil separated by a distance are used. An alternating magnetic field is generated by the alternating current passed through the Tx coil. Eddy currents are inducted in the subsurface conductive materials due to the formation of the magnetic field. In this setup, Rx coil detects the secondary magnetic field produced by the eddy currents as well as the primary field.

Typical EM systems record the quadrature phase, also known as the out-of-phase or imaginary component, and the quadrature component magnitude. The quadrature component is used to determine the apparent ground terrain conductivity. Anomalies such as filled-in abandoned channels, buried objects or voids typically produce conductivity readings which are different from the background values. The in-phase component is also very sensitive to metallic objects. Therefore, it can be very useful for locating buried metals such as metal rails, rebar, or electrical wires. However, a disadvantage is that if such materials are present and the object of the survey is not to locate such objects, these objects will interfere with the survey results

significantly. Therefore, when planning a survey, it is important to avoid locations close to metallic fences, railroads, metallic gates, etc. to ensure the conductivity readings are from the subsurface geologic materials only. Additionally, although EM induced conductivity can be used to infer information regarding mineralogy, grain size, water content and anomalies, EM units require multiple passes at different frequencies and/or different coil distances to gather data at different depths.

Figure 12 - Geonics Ltd. EM34 EM induction instrument being towed by a vehicle collecting continuous data (Llopis and Simms, 2007)

The depth of investigation in EM induction systems varies considerably based on the array type, distance between the transmitter and receiver and the operating frequency (Llopis and Simms, 2007). For example, Llopis and Simms (2007) used Geonics Ltd. EM34 induction instruments for assessing levee conditions in the Feather River levees in California. They towed

the coils on an electronically non-conductive sled at a walking distance to collect continuous data (Figure 12). The EM34 allowed for coil separations of 10, 20, or 40 m. Operating in the vertical dipole mode allowed for greater depths of investigation and less sensitivity to surface materials. This resulted in nominal depths of exploration of 15, 30 and 60 m for 10, 20 and 40 m coil distances, respectively (McNeil, 1980).Dunbar et al. (2003) conducted EM surveys in Texas by towing a symmetric and coplanar dipole system on a helicopter above the levee at an altitude of 30 m. Using different frequencies, they gathered data up to the depth of 30 m. Although this method is more rapid than other geophysical methods, it did not provide a good resolution and it is relatively expensive compared to other non-destructive methods.

#### 2.2.1.2 Ground Penetrating Radar (GPR)

Ground Penetrating Radar (GPR) is a geophysical method that images the subsurface using radar pulses. GPR transmits EM pulses (10-2000 MHz) (Davis and Annan, 1989) and the receiver antenna records the reflections. The penetration depth and resolution depend on conductivity of the materials and the signal frequency. In low conductivity materials such as dry sands, signals could penetrate up to 50 m while in conductive materials such as clays, they will penetrate only a few meters (Davis and Annan, 1989). Therefore, GPR is likely not the most effective option for levee assessment, as most levees are constructed using clays and are relatively high in water content.

#### 2.2.1.3 Light Detection and Ranging technology (LiDAR)

LiDAR uses light in the form of a pulsed laser to measure ranges (variable distances) to the earth. These light pulses, combined with other data recorded by the system, can generate

three-dimensional information about the shape of objects. These systems generally consist of a laser, a scanner and a GPS receiver (NOAA, 2017).

Palaseanu-Lovejoy et al. (2014) used LiDAR technology to create crest elevation profiles of levees in south Louisiana. They were able to identify abrupt changes in levee elevation and orientation. Using this data, they were also able to compare the levee height with the height requirements to withstand the 100-year flood. Surprisingly, only 5% of the crest points of the levees investigated passed the height requirement.

Unlike geophysical methods which provide information about the internal structure of the levee, LiDAR gives information about its geometry. This information can be used for assessing overtopping risk and slope stability analysis.

#### 2.2.1.4 Multi-channel analysis of surface waves (MASW)

There have been several cases where researchers have used MASW to assess the subsurface conditions in levees. In this method, seismic waves are created by a hammer blow or other impacts. The reflected and refracted seismic waves are recorded by an array of receivers called geophones. By analyzing the response waves and the dispersion curves, a seismic velocity profile of the subsurface can be generated. This information can be used to locate layers, infer stiffness variations and locate porous zones and voids. Shear wave velocity can also be used to determine liquefaction potential (Stokoe et al., 1988). A great example of levee assessment can be found in Miller and Ivanov (2005) where they used a range of seismic technics including MASW to test levees in Weslaco, Texas. One of the interesting findings was the applicability of the seismic tool to identify permeable areas where infiltration is active (e.g. during flood season).

In order to expedite the process of gathering seismic responses, a system called a Land streamer (Figure 13) can be used. In this setup, the geophones are in contact with the ground through a metallic plate which enables the recording of data without the need for soil penetration. Therefore, the array can be dragged behind a vehicle without the need for removal and installation of individual geophones. However, it is still required to periodically stop movement, create seismic waves using an impact source and allow a few seconds to record the data.


Figure 13 - Use of land streamer to collect seismic wave velocity data on top of a levee in Mel Price lock and Dam in Edwardsville, IL

#### 2.2.1.5 Electrical Resistivity Methods

Electrical resistivity is an intrinsic property that quantifies how strongly any given material opposes the flow of electrical current. The use of the electrical resistivity method has a long history in geophysical testing and it was made famous through the pioneering work of Conrad Schlumberger in France in 1912. (Dahlin, 2001).

Electrical resistivity measurements require at least four-electrodes, two current electrodes and two voltage potential electrodes. The arrangement of the electrodes and sequence of measurements is the array and many different arrays have been developed through the years. For example, to measure the electrical resistivity using a Wenner array (Figure 14 (a)), electrical current is passed between two external electrodes inserted into the ground (current electrodes) and then the resulting voltage potential is measured across two internal electrodes inserted into the ground (potential electrodes) (Herman, 2001). Some of the most common resistivity arrays are shown in Figure 14.

In the DC electrical resistivity method, the electric current $I$ is directly injected into the ground through a pair of electrodes and the resulting voltage $V$ is measured between a second pair of electrodes. The impedance $Z = V/I$ is calculated which is then transformed into apparent resistivity $\rho_a$ which is an indicator of the underlying resistivity structure $\rho(r)$ of the earth. (Everette, 2013). The depth of a resistivity measurement depends on the distance between the current or sink electrodes and the distance from the voltage potential electrodes. Each measurement is called the apparent resistivity and is the measurement that would have been measured if the entire subsurface was uniform (Everett, 2013). A map of the apparent resistivity plotted at these locations is termed a pseudosection (Loke, 1999).

Construction of a pseudosection using a diploe-dipole array (Figure 14 (d)) is shown in Figure 15; where the measured apparent resistivity associated with current AB and potential electrode pairs PQ is plotted at the intersection of two 45° angles passing through the center of the electrode pairs. By moving the electrode pairs, apparent resistivity is measured at different depths and locations. (Everette, 2013). However, the pseudosection only provides a rough estimate of the true resistivity of the subsurface. Through a process called inversion, which requires complex mathematical calculations, true resistivity of the ground is obtained (Figure 16).

#### 2.2.1.5.1 Electrical resistivity tomography (ERT)

An electrical resistivity sounding in which the electrode spacings are varied without moving the midpoint, provides a local 1-D electrical resistivity depth model at midpoint, $\rho(z)$. By traversing the array over a horizontal profile without altering the electrode spacings, lateral profiling of $\rho(x)$ over a limited depth range can be achieved. However, this method faces several challenges in complex geologies (Everette, 2013).

#### 2.2.1.5.2 Capacitively coupled resistivity (CCR)

A relatively rapid method to collect electrical resistivity data in the field is using Capacitively Coupled Resistivity (CCR). A geometrics OhmMapper (Figure 17) uses one transmitter and 5 receivers. The spacing between the transmitter and the first receiver and the spacing between each receiver can be modified to allow for resistivity measurements at different depths. An advantage of this system is that unlike the conventional DC electrical resistivity methods, CCR does not require direct contact with the ground (Chlaib, 2014). This offers two advantages, as it reduces the setup time for subsequent measurements and enables measurement

on hard surfaces such as pavements where electrode penetration is not possible or desired. The OhmMapper can be dragged behind a vehicle or by humans at walking speed (approximately 2 km/hr) while the system continuously collects data and builds the pseudosection using the GPS data in real time. However, depending on the target of the investigation, multiple passes may be needed to gather data at different depths. Larger spacings correspond with deeper measurements but lower resolution, similar to any other geophysical method.

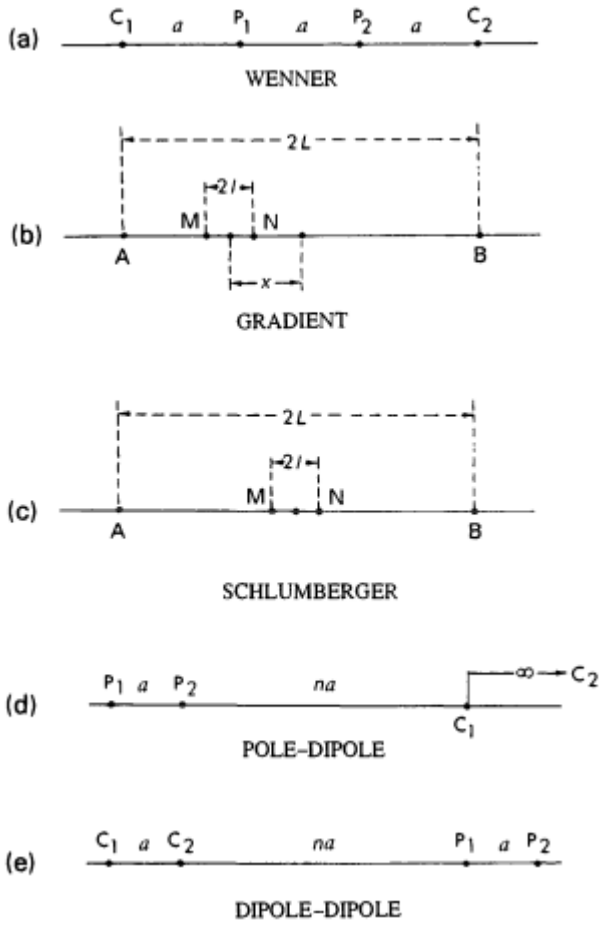


Figure 14 - commonly used electrode arrays in resistivity surveys. C1, C2 and P1, P2 denote the position of the current and potential electrodes. For the symmetrical and gradient Schlumberger arrays, it is common to use symbols A, B for the current electrodes and M, N for the potential electrodes. (Sharma, 1997)

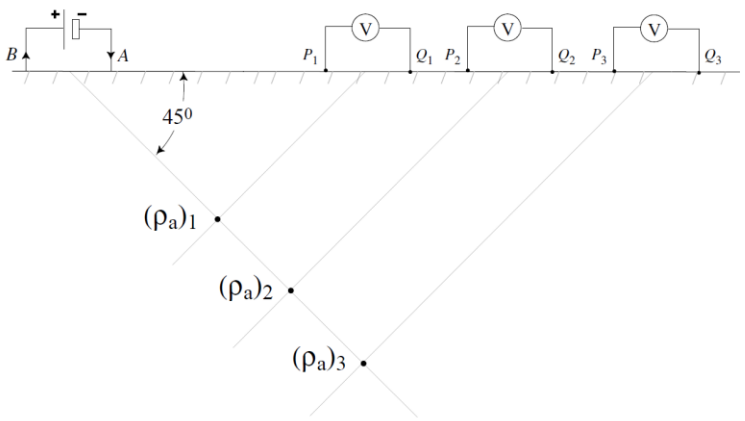


Figure 15 - Construction of a dipole-dipole resistivity pseudosection (Everette, 2013)

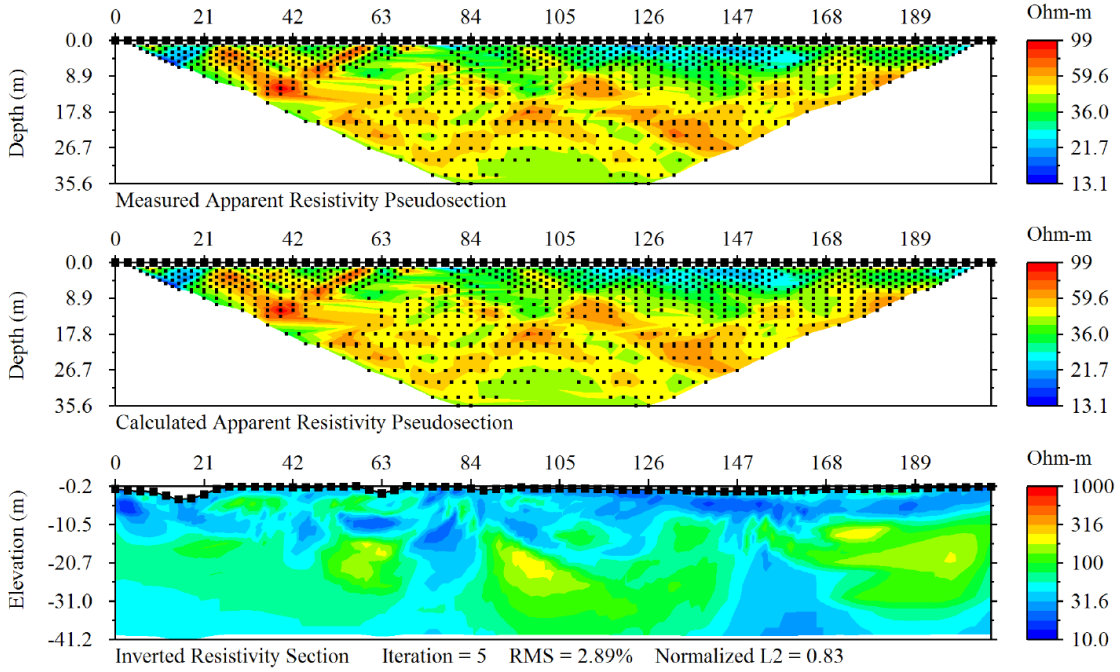


Figure 16 - measured apparent resistivity pseudosection for a hybrid Schlumberger – dipole-dipole electrode configuration (Top) along with the inverted resistivity image (Bottom). Middle image shows the calculated apparent resistivity based on the inverted cross section. (Everette, 2013)

Figure 17 - CCR used to measure electrical resistivity at the toe of a levee close to the Mel Price Lock and Dam in Edwardsville, IL

## 2.3 Selection of Methods for the Current Study

As discussed, there are many non-destructive testing options available to assess levees. Although LiDAR does not provide any information about the subsurface conditions, it is an effective tool to assess overtopping and find surficial defects. Although several researchers have used GPR for levee assessment, it is not as effective for deep investigations in clay filled structures despite having a relatively high resolution in sands and gravels. In other words, although GPR may be able to capture information within the levee itself, it would likely not be able to detect any of the foundation soils along the center of the levee. EM methods enable

measurement of the electrical conductivity of subsurface; however, these systems only use one transmitter and receiver whereas, electrical resistivity methods use an array of receivers and transmitters to measure the resistivity. Multiple receivers enable the measurement of apparent resistivity in several depths simultaneously which results in a fewer of number of passes. In this sense, electrical resistivity has an advantage over EM. MASW is also a powerful tool in assessing subsurface conditions, as it can incorporate different types of seismic waves to measure elastic properties of the soils (e.g. P-Wave, S-Wave, and Rayleigh wave velocity) which cannot be directly measured by any of the other methods. However, this method also has shortcomings. For example, a loose sand may have a similar velocity to a dense clay deposit. This could lead to erroneous conclusions of levee conditions because a dense clay is very desirable for levees, while the loose sand is highly susceptible to erosion and it may not be clear to distinguish the two.

Seeing the advantages and disadvantages of different testing methods for assessing subsurface conditions, it was decided that both MASW and electrical resistivity should be used in conjunction with each other. Hayashi and Konishi (2010) proposed an integrated geophysical method using electrical resistivity and surface-wave methods in conjunction with each other to evaluate vulnerable points of levees in Japan. The authors were able to develop a matrix to detect the presence of alluvial and diluvial gravel and alluvial sand and clay deposits using the two methods together. Their research indicated that resistivity increases with decreasing density and increasing grain size, while S-Wave velocity decreases under those conditions. The basic concept behind this assessment method is depicted in Figure 18. Similarly, Hayashi et al. (2014) developed a polynomial equation using cross-plots of S-Wave and resistivity to estimate soil

parameters, such as fines content, $D_{20}$, SPT blow count, and general soil type descriptors (e.g., sand, clay, gravel).

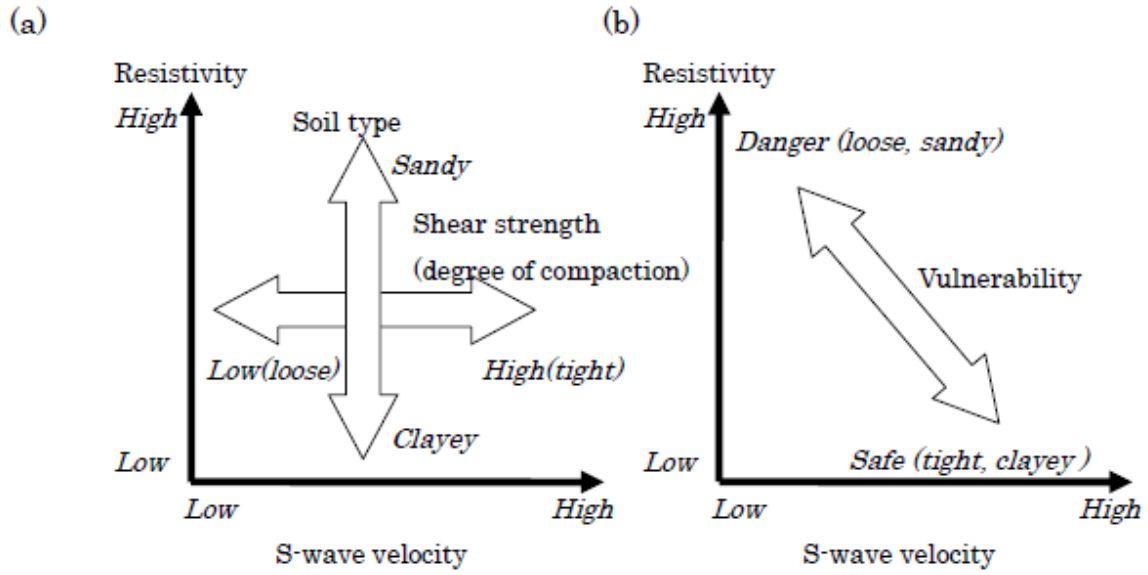


Figure 18 - Schematic relationship between geophysical properties and soil condition (a) and levee vulnerability (b) (Hayashi and Konishi, 2010)

This thesis is portion of larger study where electrical resistivity and MASW were used to develop a framework for rapid and non-destructive assessment of levees. While field measurements were taken using CCR, it was determined that a laboratory study would be more effective in order to avoid the large variability observed for natural soils in the field. This thesis focuses on the electrical resistivity portion of the study and uses controlled laboratory measurements to examine the relationship between electrical resistivity and parameters such as water content, temperature, water composition, etc. The ultimate goal was to develop relationships in order to predict soil type from field based measurements of resistivity.

## 2.4 Previous Resistivity Studies Aimed at Determining Soil Type

There have been many attempts to identify soil type based on its resistivity magnitude. Piegari and Di Maio (2013) were able to derive an empirical relationship between soil resistivity and suction using a combination of Archie (1942) and Van Gnuchten (1980) models on a series of laboratory and field experiments. According to the field studies conducted by Besson et al (2004), electrical resistivity can be used to describe the structure of the tilled soil. Additionally, Seladji et al. (2010) investigated the effect of soil compaction on electrical resistivity in a series laboratory experiments. The authors focused on agricultural samples of clay and loam with organic content and analyzed the effect of soil microstructure, organic matter and saturation level on the measured electrical resistivity. While they were able to fit a model to their results, the results indicated a further need for investigation of low saturation soils and the effects of organic matter on the electrical resistivity of soil.

There have also been several efforts to relate field resistivity measurements to soil type or soil classifications. Two of the more significant studies were conducted by Kaufman and Hoekstra (2001) and Palacky (1987). Their results are summarized in Table 2.

Table 2- Resistivity ranges of different soil types

| Soil Type | Soil Classification | Resistivity (Ω.cm) (Kaufman and Hoekstra, 2001) | Resistivity (Ω.cm) (Palacky, 1987) |
|---|---|---|---|
| CLAYS | CH | 1,000-5,000 | 300-10,000 |
| | CL | 2,400-6,000 | - |
| | OL | 2,650-7,500 | - |
| SILTS | ML | 2,650-7,250 | - |
| | SC | 4,650-17,800 | - |
| | MH | 7,150-24,000 | - |
| SAND | SM | 9,600-45,250 | 47,500-1000,000 |
| GRAVEL | GW | 56,300-91,800 | 47,500-1,000,000 |
| | GC | 12,900-40,500 | - |
| | GP | 91,500-233,250 | - |

According to Kaufman and Hoekstra (2001), there are overlaps between many of the different soil types. Moreover, Palacky (1987) published a different range of values for similar soil types. He measured much lower resistivity values for clays, while his measured lower bound resistivity for sand surpassed the upper bound resistivity measured for sand by Kaufman and Hoekstra (2001). According to Palacky, gravels can have much higher resistivity compared to what was published by Kaufman and Hoekstra (2001). These two publications show some of the complexity of deriving soil type and geotechnical properties from electrical resistivity data measured in the field.

As discussed, many researchers have worked over the past seven decades to interpret the results of non-destructive geophysical testing methods for engineering purposes. Most of these researchers conclude that there is a need for more work in this area (Seladji et al., 2010, Samouelian et al., 2005, Piegari and Di Maio 2013). As it is very challenging to understand the effect of various geotechnical parameters on electrical resistivity using field measurements where soils can be highly variable, the resistivity of different benchmark soils was measured

under controlled laboratory conditions. A laboratory investigation of resistivity provided the opportunity to examine the effect of temperature, water quality, soil type, density and water content to better understand the range of resistivity values possible for a particular soil. The methodology of this research is described in the following chapter.

## Chapter 3: Research methodology

To measure the electrical resistivity of the soil, a Nilsson Resistance Meter Model 400 attached to a M.C. Miller Large Soil Box in a Wenner 4-electrode array (Figure 19) was used. According to ASTM G57 - 06(2012), the electrical resistivity of a soil specimen in this configuration is

$$\rho = R \cdot A/a \qquad \text{Eq. 1}$$

where R is the electrical resistance measured between the two inner electrodes in Ohms (Ω), A is the cross-section of the soil specimen in $cm^2$ and a is the distance between the inner electrodes in cm. For the soil box used, the distance between the inner electrodes is 12.8 cm and the cross section is 12.8 $cm^2$ which gives the cross section to length ratio (A/a) of 1 cm. For this setup, the magnitude of the measured electrical resistance (R) in Ω is the same as the magnitude of its electrical resistivity (ρ) in Ω.cm. To ensure consistency in measurements and control over parameters such as density, water content and degree of saturation, the following procedures were followed.

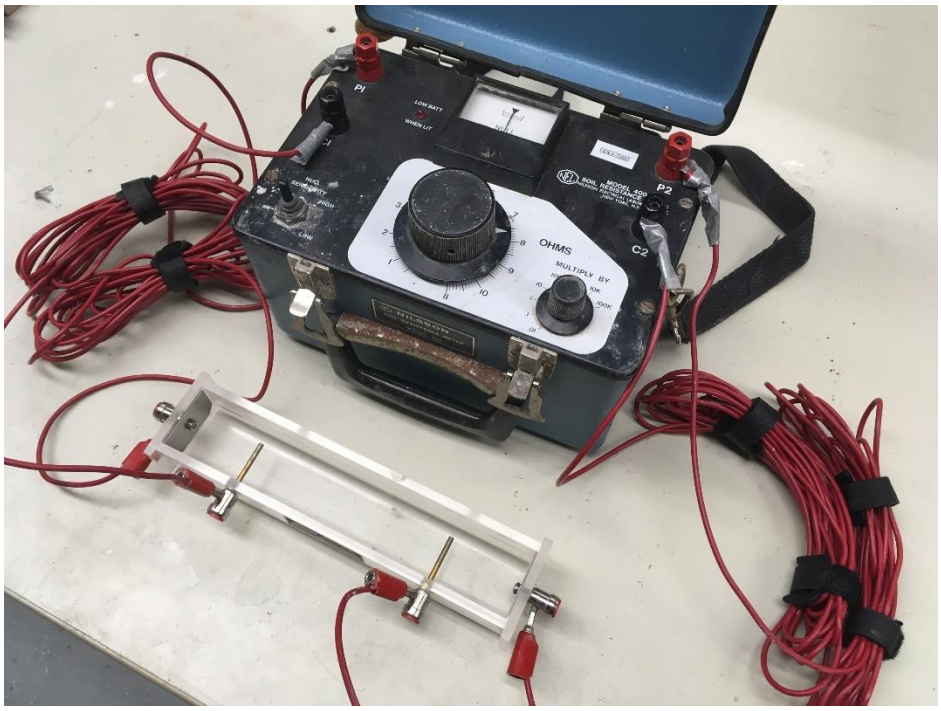


Figure 19 - Resistivity measurement setup

First, the water and dry soil mass were measured with a scale accurate to 0.01 g and were mixed thoroughly. The mixed soil was then sealed in a container and kept for at least 24 hours in a room with controlled temperature and humidity. To ensure the soil was at the target water content, it was weighed at the end of mixing and once more before the start of the test. A sample was also taken at the end of the test to verify the water content. Because of the many variables affecting electrical resistivity, it was critical to ensure that the specimen in the soil box was as uniformly placed as possible. To hit target densities, the total amount of the soil required to fill the box was calculated and placed in three equal layers. Once filled, the total weight of the soil box was recorded for final density calculations and then the electrical resistivity and temperature of the specimen were measured simultaneously three times and then averaged. As soil temperature increases, its electrical resistivity decreases. Therefore, all of the resistivity values

presented in this paper have been corrected to a common temperature of 15.5° C following Eq. 2 from ASTM G57-06 (2012)

$$\rho_{15.5}=\rho_t\ ((24.5+T)/40) \qquad \text{Eq. 2}$$

where T is the temperature of the soil at the time of measurement and $\rho_t$ is the resistivity of the soil at that temperature. $\rho_{15.5}$ is the corrected resistivity value at 15.5° C.

A total of nine different benchmark soils were made by mixing different portions of commercially available sand, Kaolin clay, Bentonite clay and red art clay. Deionized water was used for all of the tests to ensure repeatability. In Table 3, the composition of each benchmark soil is shown along with the measured index properties, as well as the range of densities and water contents in which each was tested. For the electrical resistivity measurements, each soil was tested at its loosest and densest possible compacted states corresponding to various water contents. Additional intermediate densities were also tested to obtain a representation of how electrical resistivity varies with density and water content. The dry density and corresponding water contents for the points tested are shown in Figure 20, where each benchmark soil is assigned a label according to its group symbol from USCS (ASTM D2487-11). The water content was varied from the driest possible state to a very wet state where electrical resistivity did not change with increased water content (AASHTO Standard T 288-12, 2012). The lowest tested water content for each soil type was limited by the equipment's maximum measurable electrical resistivity (1.1×106 Ω.cm) and was different for each soil type according to their physical properties. For example, the electrical resistivity of the poorly graded sand (SP) is measurable at a water content of 2% while the high plasticity silt (MH) required a water content

of at least 6% for its electrical resistivity to be measurable using the current setup. The majority of soils in the field will likely be at water contents well above these thresholds.

Because it is known that the electrical resistivity of soil is a function of the resistivity of pore fluid, the effect of water composition was explored by comparing resistivity values for a common soil mixture with different water sources: distilled water, tap water from Arkansas, ground water from a well in Texas and ground water from a well in Arkansas. However, to ensure the consistency and reproducibility of the results for future studies, the remainder of the tests were carried out using deionized water.

As shown by Eq. 2, temperature is also known to affect the electrical resistance of different materials. In materials classified as conductors (e.g. copper), an increase in temperature is expected to increase the electrical resistance and in materials classified as insulators (e.g. glass), the opposite effect is observed. Since soils are mainly composed of insulators such as silicates, they are expected to have lower electrical resistivity at higher temperatures. To measure resistivity at different temperatures, the soil sample was compacted in the soil box, sealed and stored in a cold storage room until it reached the room temperature (5 °C), then it was removed from the room and tested continuously until it reached the ambient room temperature (21 °C). To measure electrical resistivity at higher temperatures, the sealed soil box was put in an oven at 30-40 °C for a short time. Once at equilibrium, the soil was removed and tested until it reached the ambient room temperatures again. It was important to cover the soil tightly between tests and while waiting to reach the target temperatures to avoid evaporation as much as possible.

Table 3 - Material description, index properties, and density and moisture conditions for the soils tested

| Soil Type | Composition (% mass) | | | | Index Properties | | | | | | | Testing range | |
|---|---|---|---|---|---|---|---|---|---|---|---|---|---|
| | Sand | Kaolinite | Bentonite | Red Art Clay | LL (%) | PL (%) | PI (%) | Gs | $D_{90}$ (μm) | $D_{50}$ (μm) | $D_{10}$ (μm) | Bulk Density ($kg/m^3$) $\times 10^3$ | w (%) |
| SP | 100 | 0 | 0 | 0 | - | - | - | 2.67 | 850 | 440 | 240 | 1.63-2.00 | 2-20 |
| SP-SM | 90 | 10 | 0 | 0 | - | - | - | 2.66 | 800 | 380 | 100 | 1.12-2.11 | 4-16 |
| SP-SC | 90 | 8.5 | 1.5 | 0 | - | - | - | 2.64 | 780 | 375 | 80 | 0.98-2.10 | 3-12 |
| SC | 70 | 25.5 | 4.5 | 0 | 28 | 15 | 13 | 2.70 | 730 | 320 | - | 1.09-2.15 | 4-18 |
| SM | 70 | 30 | 0 | 0 | 26 | 15 | 11 | 2.64 | 750 | 330 | - | 1.03-2.11 | 10-15 |
| CL-1 | 0 | 0 | 0 | 100 | 38 | 19 | 19 | 2.77 | 25.4 | 7.8 | 0.49 | 1.13-2.10 | 2-39 |
| CH | 0 | 85 | 15 | 0 | 72 | 33 | 39 | 2.62 | 6.6 | 0.4 | - | 1.15-1.82 | 10-60 |
| CL-2 | 30 | 70 | 0 | 0 | 48 | 24 | 24 | 2.60 | 550 | 1.8 | - | 1.06-1.94 | 14-30 |
| MH | 0 | 100 | 0 | 0 | 62 | 32 | 30 | 2.61 | 5.9 | 0.4 | - | 1.06-1.60 | 6-70 |

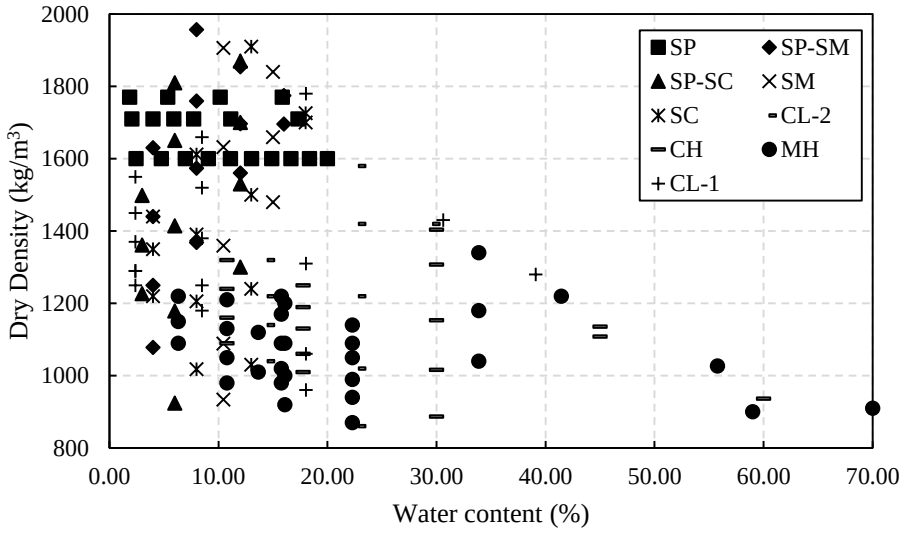


Figure 20 - Dry densities and corresponding water contents tested

## Chapter 4: Results and Discussion

As discussed several geotechnical parameters were examined to better understand their effects on the resistivity of different soils. Along with measuring the resistivity of different soil

types according to the USCS, the effects of water composition, temperature, density, saturation and volumetric water content are also investigated.

### 4.1 Water composition

The variation of electrical resistivity for the SP soil using different water sources and saturations is presented in Table 4. Degree of saturation greatly influences the electrical resistivity, regardless of water composition; electrical resistivity changing from approximately 90,000 to 7,000 ohm.cm from 10% saturation to fully saturated condition. As shown in Table 4, deionized water results in the highest resistivity as it introduces the least amount of ions to the mixture. The smallest resistivity measurement was measured for the well water from Texas. Another interesting observation is that while pore water composition significantly affects the resistivity at low degrees of saturation, it does not seem to play a major role when the sand is saturated. As shown, using deionized water results in the highest resistivity measurements, which should be taken into account when natural soils are tested and compared to the benchmark samples.

Table 4 - Effect of water type on resistivity of sand (SP) ($\gamma d$ = 1600 kg/m3)

| Water Type | Saturation (%) | Resistivity (Ω.cm) |
|---|---|---|
| Distilled Water | 10 | 93000 |
| Tap water - Arkansas | 10 | 88000 |
| Well water- Arkansas | 10 | 80000 |
| Well Water - Texas | 10 | 75000 |
| Distilled Water | 100 | 7520 |
| Tap water - Arkansas | 100 | 7500 |
| Well water- Arkansas | 100 | 7400 |
| Well Water - Texas | 100 | 7110 |

## 4.2 Temperature

The effect of temperature on the resistivity of two different soil types (SP and SP-SM) is shown in Figure 21, where the points represent the laboratory measurements and the dotted line represents the prediction of Eq. 2 based on the resistivity estimate at 15.5 °C.

It can be seen that there are slight deviations from Eq. 2 for temperatures lower than 10 °C; however, the relationship works well for the ambient laboratory temperatures at which the rest of the measurements were taken in this study (15-23 °C).

Based on the data, a decrease in temperature from 20 °C to 5 °C can increase the resistivity by roughly 50%. Therefore, all of the values reported in the following sections have been transformed to the equivalent resistivity value at 15.5 °C using Eq. 2. Seeing the effect of temperature on electrical resistivity, it is recommended that the temperature in the field be approximated for any future studies aiming to interpret field measurements using laboratory data. The electrical resistivity data presented in the following section is the resistivity at 15.5 °C while in the field, a range of temperatures can be experienced depending on parameters such as seasonal and daily changes in solar radiation, slope orientation, thermal conductivity of soil, water content and vegetation cover (Florides & Kalogirou, 2005). Despite its complexity, there are several models available in the literature which can help estimate ground temperature at various depths in different seasons such as those presented by Mihalakakou et al. (1997) and Kusuda & Achenbach (1965).

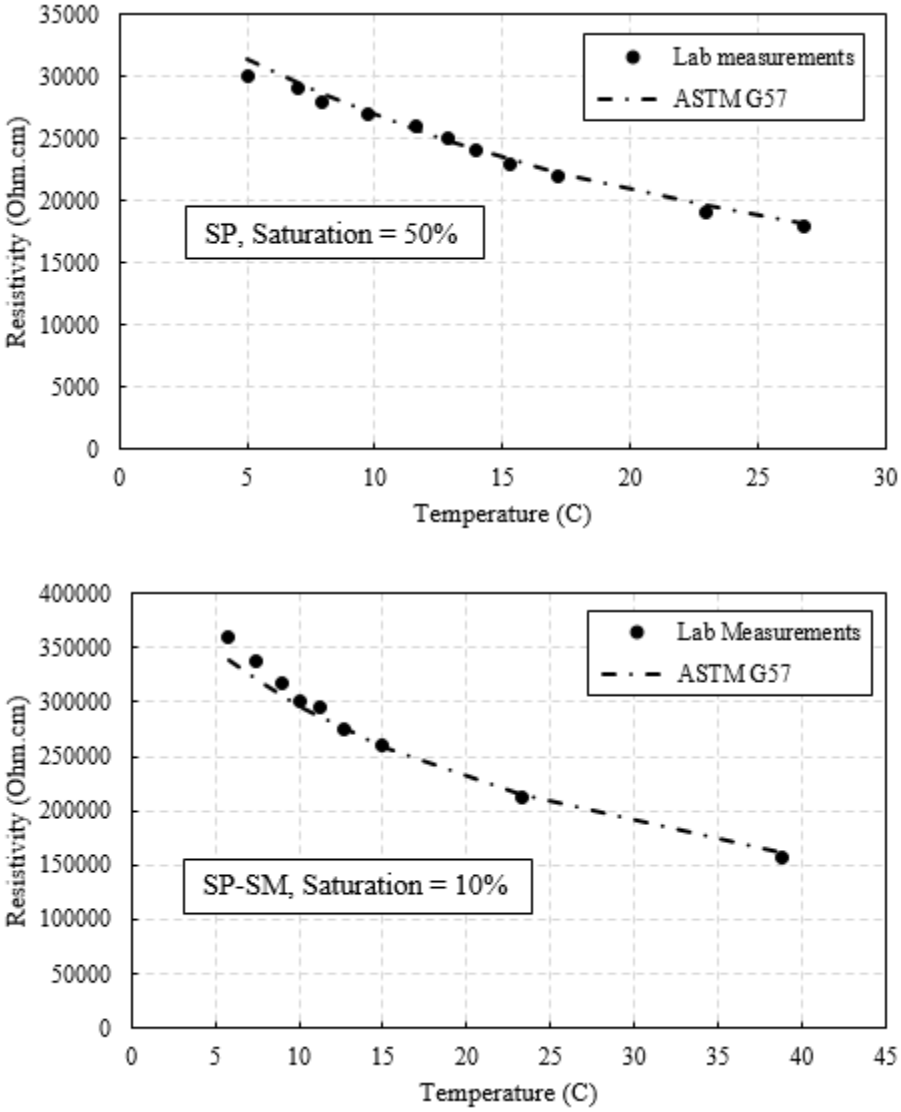


Figure 21 - Effect of temperature on resistivity

### 4.3 Degree of saturation, dry density, bulk density, and volumetric water content

As discussed, each soil was tested at various combinations of densities and water content, which resulted in several options for plotting the data. Resistivity values were plotted versus the degree of saturation, bulk density, dry density, and the volumetric water content to examine how the electrical resistivity measurements were influenced by moisture and density and to identify any

trends (Figure 22). Plotting these various combinations was also important because of the large range of possible resistivity values for a given soil type.

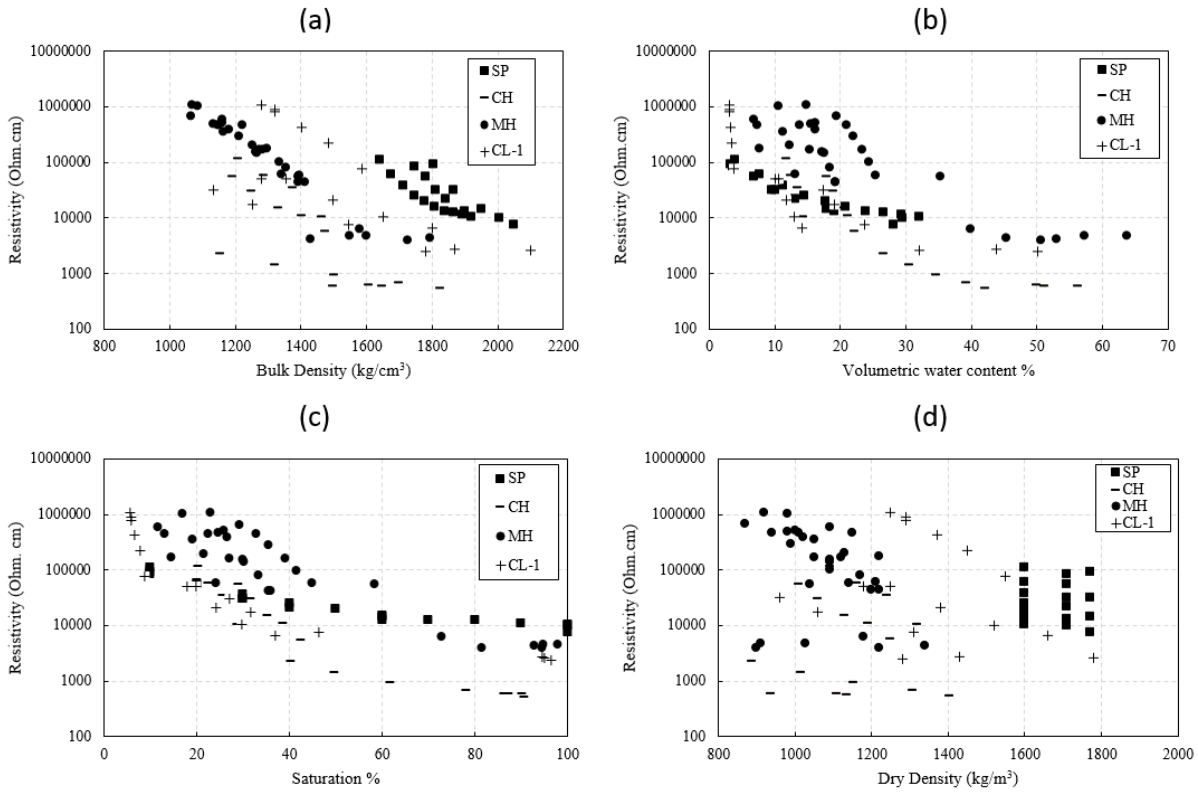


Figure 22 - Effect of bulk density (a), volumetric water content (b), saturation (c) and dry density (d) on resistivity of different soils

The bulk density and corresponding resistivity results for SP, CL-1, CH and MH soil types are displayed in Figure 22 (a). As can be seen, the non-plastic soil type (SP) lies in the upper right boundary of the plotted results while the soil type with highest PI (CH) occupies the lower left side of the plotted data and the MH and CL-1 soils occupy the area in between. The MH soil type has a higher PI than CL-1 (Table 3) and in Figure 22 (a) generally lies closer to the CH soil as compared to CL-1. Although some of these soils overlap each other in some locations, there appears to be a correlation between PI and the parameters plotted in Figure 22 (a). This likely indicates that bulk density could be used as a parameter for predicting soil type for soils

that are not in a saturated condition. One disadvantage of this parameter from a field testing standpoint is that it would require some measure of in situ bulk density to single out a soil type, which requires another test to be conducted.

The relationship between resistivity and volumetric water content was also investigated (Figure 22 (b)). As can be seen, soils have a big range of resistivity for volumetric water contents below 25%. However, the effect of volumetric water content becomes limited on electrical resistivity for water contents above 30%. Although generally electrical resistivity decreases with an increase in volumetric water content, it cannot be concluded that the sample with lower electrical resistivity necessarily has higher volumetric water content. This is especially true for silts and clays where the minimum electrical resistivity (at saturation) is lower than the electrical resistivity of water alone. Moreover, it can be seen in Figure 22 (b) that the different soil types plot very close to each other when volumetric water content is used. Therefore, although volumetric water content provides a better correlation with resistivity in comparison with dry density, it would still be hard to identify the type of soil based on this parameter.

As shown in Figure 22 (c), an increase in the degree of saturation leads to a decrease in resistivity for all soil types. Additionally, the minimum recorded resistivity for each soil (generally for degrees of saturation above 60%) decreases as its plasticity index (PI) increases. For example, the minimum resistivity observed for the high plasticity clay (CH) which has the highest PI is much lower than the minimum resistivity observed for the other soils tested. This

trend could potentially help distinguish between high and low plasticity soils in saturated or close to saturated conditions.

The resistivity values were also plotted with the corresponding dry densities (Figure 22 (d)). It is evident from Figure 22 (d) that there is little correlation between dry density and the resistivity of soil since a soil's resistivity can vary several orders of magnitude at a specific dry density due to change in water content. Therefore, even if the dry density were known, it would be impossible to identify the soil based on its resistivity and dry density alone.

Although the dry density alone would not be a good indicator, it was proposed that a combination of degree of saturation and dry density might give the necessary information to distinguish between soil types. The effect of saturation and dry density on the resistivity of SP, CH, MH and CL-1 soils is shown in Figure 23. It shows that although the saturation is the major factor that affects resistivity, some soils are heavily influenced by their dry density (e.g. MH), whereas some are minimally affected by it (e.g. SP). Another important observation is that for each soil, there appears to be a limit saturation level above which the resistivity does not change significantly. At this level, dry density also does not affect the resistivity, which indicates that different densities could not be identified for a given soil in a saturated condition.

More importantly, these plots show that soil type could be narrowed down significantly if resistivity were known for the soil in its saturated condition. For example, a saturated sample with a resistivity value near or above 10,000 Ω.cm would likely be a sand and a saturated sample with a resistivity value below 1,000 Ω.cm would likely be a CH. This saturated condition could be assumed for soils below the water table and could perhaps be useful for non-destructive field-testing. The difference in the resistivity values for the saturated MH and the saturated CL-1 is not

as well defined; however, the difference in the resistivity values at high and low saturation levels is drastically different. Therefore, identifying a particular soil is much more likely if resistivity values were known at two drastically different saturation levels (i.e. at perhaps 20% and 60% or greater). While this is easy to do in the laboratory, it is not as practical in the field, especially for soils below the water table.

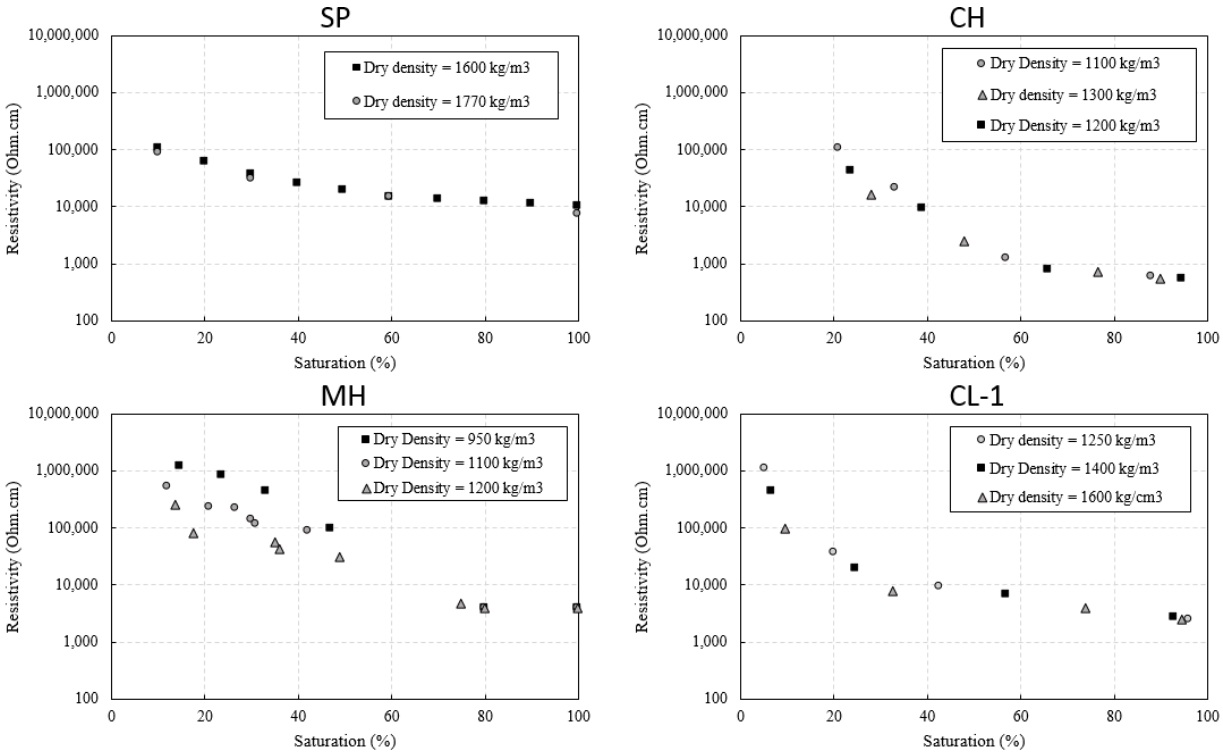


Figure 23 - Effect of saturation on different soil types at different dry densities

Although some correlation between each parameter and the measured resistivity is observed, the two parameters that were determined to be the most effective in identifying soil type were the degree of saturation and the bulk density. The best estimate of soil type can be made by using a combination of these two parameters and the corresponding resistivity values. To demonstrate this, the bulk density plot (Figure 22 (a)) was regenerated and the samples with the highest and lowest saturation values were identified using hollow markers and labels of the

percent degree of saturation. While it was not true for all the soil types, highest and lowest saturations typically corresponded with some of the highest and lowest bulk densities. As shown in Figure 24, the regions for each of the various soil types is well defined with only a few samples as exceptions. The diagonally oriented zones move from right to left as PI increases. The results indicate that soil type can be greatly narrowed down and even possibly identified if even an estimate of the degree of saturation and/or bulk density can be made.

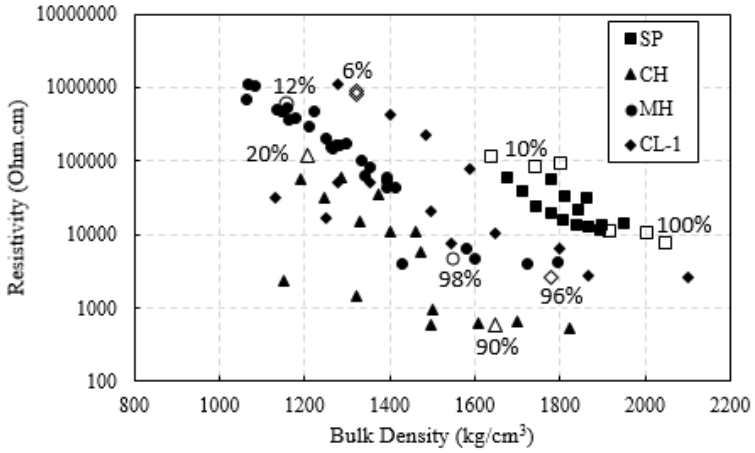


Figure 24 – Comparison of resistivity values and corresponding bulk density and saturation values (numbers inside the plotting area indicate degree of saturation for the hollowed out symbols)

As seen in Table 3, some soils were made by mixing different proportions of sand and Kaolin clay or sand, Kaolin clay and Bentonite clay to obtain the different major group classifications according to USCS. The resistivity measurements for SP,SP-SM, SM, MH and CL-2, i.e. Sand-Kaolin clay mixes, are shown in Figure 25. When resistivity is plotted as a function of bulk density, the SP soil type is somewhat separated from the other soils (Figure 25 (a)). Considering the samples with higher bulk densities, the resistivity values decrease as the fines content of the mixes increase. Figure 25 (b) shows that if the degree of saturation is known, it is possible to distinguish soil type using resistivity. As can be seen, if the soil is saturated under approximately

60%, the higher the fines content, the higher its electrical resistivity will be. However, close to saturation this relationship is inversed and soils with higher fines content show less electrical resistivity. This is because when Kaolin clay is relatively dry and in powder from, it has many air voids that increases the resistivity of the material. However, as the water content increases, ions will be able to travel more freely in the pore spaces, resulting in a lower resistivity. Therefore, the difference between the resistivity values of these mixes in a saturated condition is likely attributed to the difference in their mineralogy, while the difference in resistivity values in a drier condition is likely more related to the air void volume.

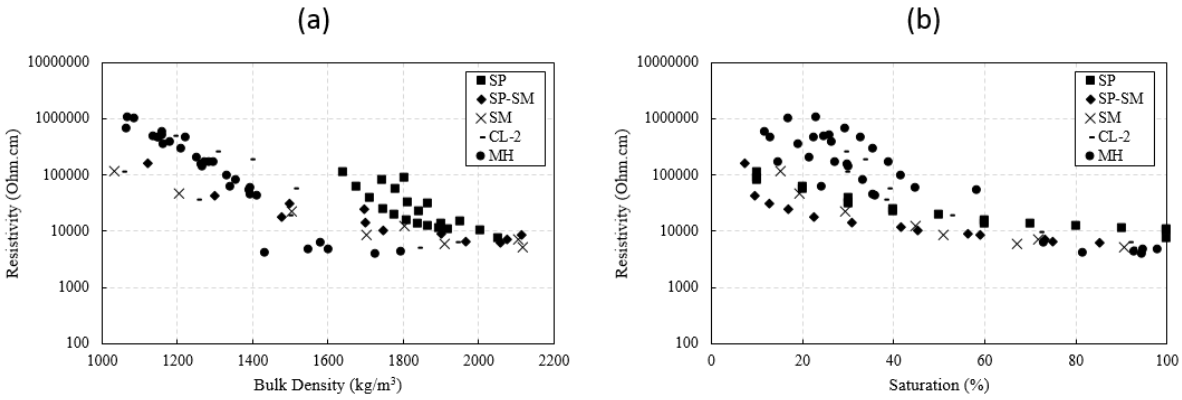


Figure 25 - Resistivity of Sand – Kaolin clay mixes with respect to bulk density (a) and degree of saturation (b)

The results for Sand-Kaolin clay-Bentonite clay mixes are displayed in Figure 26. A similar correlation is observed where SP (Sand) and CH (Kaolin clay-Bentonite clay) are the clear outliers at relatively high bulk densities and saturations. In general, for the bulk density data, higher plasticity soils tend to plot closer to the lower left corner while non-plastic soils plot

to the upper right. Although a large number of benchmark samples were tested, it is important to examine these findings further using several natural soils.

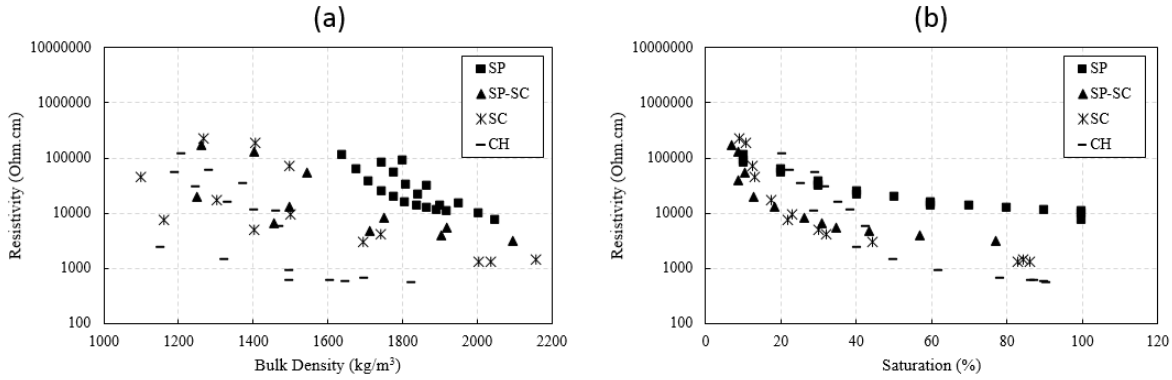


Figure 26 – Resistivity of Sand-Kaolin clay-Bentonite clay mixes with respect to bulk density (a) and degree of saturation (b)

### 4.4 Verification studies

Three cases were considered to assess the practicality of using the benchmark soil data in identifying soil types for natural field retrieved soil samples. For the first case, a clay sample obtained in Monticello, AR was considered. The soil was compacted in the soil box at the natural water content of 36.17 % to a bulk density of 1890 kg/m3, similar to the measured in situ bulk density (1878 kg/m3). The measured resistivity was 617 Ohm.cm. From Figure 22, it is evident that only a CH soil type has a resistivity lower than 1000 Ohm.cm. The sample indeed classified as a CH and neither water content nor density were necessary to determine the soil type for this sample because of the significantly low value of resistivity.

For the second case, a natural clay sample was tested at a water content of 8.35% and at densities of 1125.9 kg/m3 and 1415.37 kg/m3. The measured resistivities were 70,050 and 11,832, respectively for the two cases. Following the suggestions above, the sample was also tested at a higher water content of 36.01% and a bulk density of 1701.4 kg/m3 and the resistivity

was found to be 1,504. Figure 27 shows these samples plotted with the benchmark sample results. The classification can be narrowed down to either a CL or CH based on the first two points. Considering the third point at the more saturated condition, the sample would likely be a CL. The sample actually classified as a CL, with a liquid limit of 36 and a plasticity index of 16. Therefore, the benchmark samples also appear to provide a means of identifying the classification for soils falling within the more difficult range. While the moisture content and densities can be varied for a field retrieved sample, examining a soil at different densities would be impractical in a single field study. These types of comparisons were simply made to examine the ability of the developed plots to capture soil type, similar to a blind study. As more and more natural samples are added in the future and adjustments are made to the relationships, it is likely that a clearer distinction could be made.

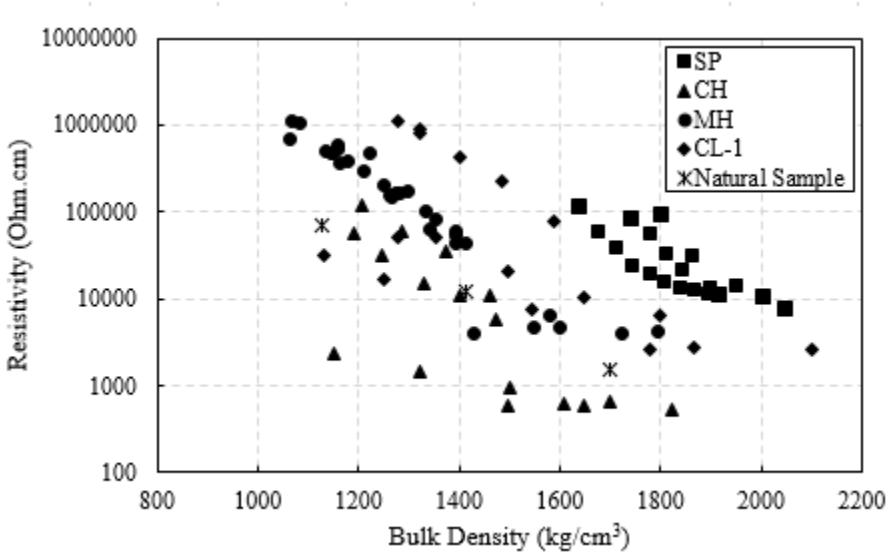


Figure 27 – Results of the natural soil sample plotted along with other major soil types

For the third case, a natural soil known as Hillside red clay (common in Arkansas) was investigated. This soil is generally a mixture of red clay and fragile cobbles of chert. The soil was sieved using a #10 sieve to separate the larger pieces of rock. The resulting sample had a

fines content of 92.60%. The liquid limit was found to be 66 and the plasticity index was found to be 37, resulting in a USCS classification of CH. The resistivity of the soil was measured at a relatively high water content (+35%) The results of these tests along with the results obtained for other major soil types are presented in Figure 28.

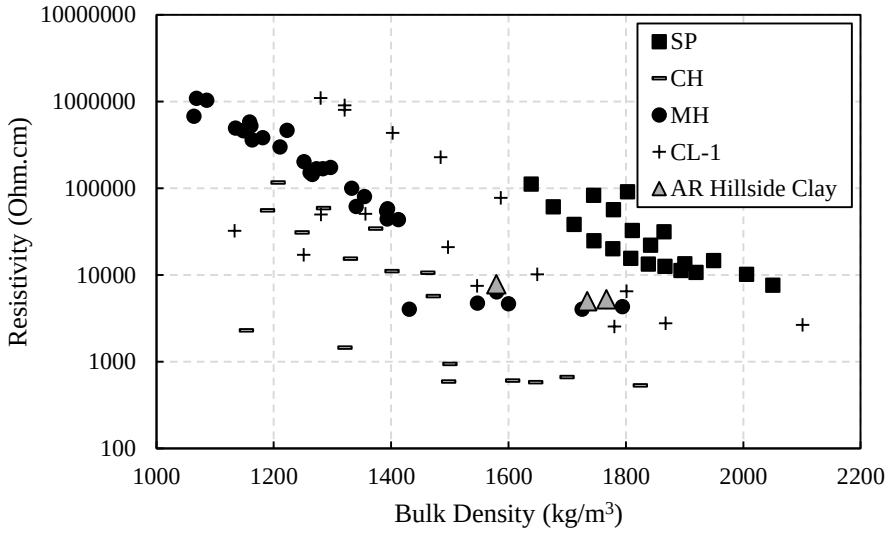


Figure 28 - Results of the Arkansas Hillside clay plotted along with other major soil types

Despite the CH classification, it can be seen that this soil overlaps the results of the MH benchmark sample. A comparison of the Atterberg limits of the three soils on the typical plasticity chart reveals that they are all very near the A-Line (Figure 29). However, one of the main reasons this soil behaves like a MH according to the resistivity measurements may be due to the existence of small grains of chert mixed with the red clay.

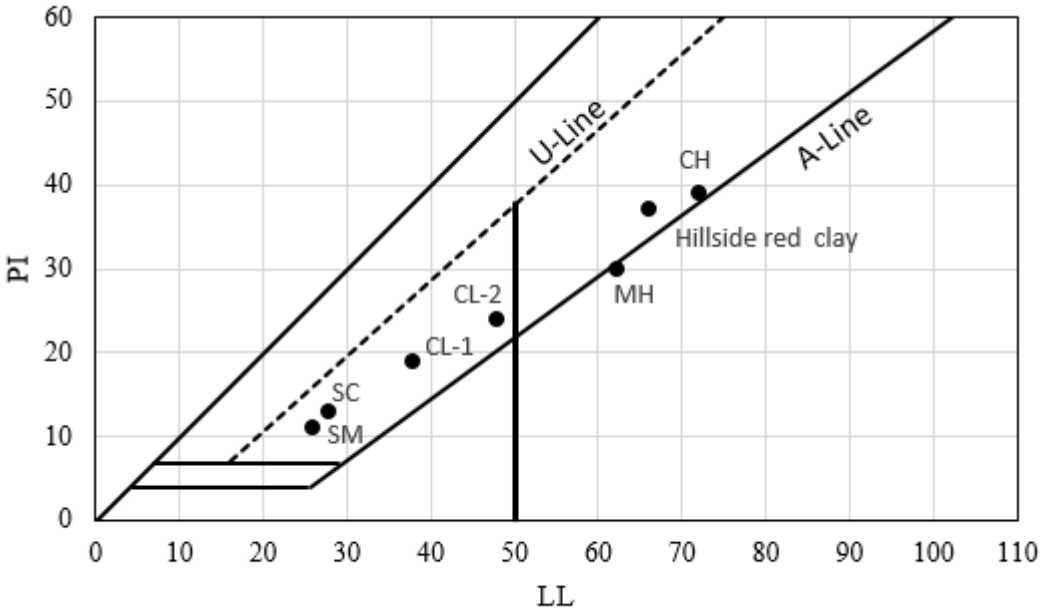


Figure 29 - Atterberg limits of different soil types used in this study

For the third case, two different sands, designated as SP-1 and SP-2, from Arkansas were tested at high and low water contents and densities. It was observed that these soils show higher resistivities (10,000-20,000 ohm.cm higher) compared to the benchmark SP sample when saturated. However, it is still evident from Figure 30 that these two cases lie closest to the benchmark SP sample compared to the other soil types. It is likely that the higher resistivity measurements may be due to slight difference in mineral composition, gradation and perhaps even fines content.

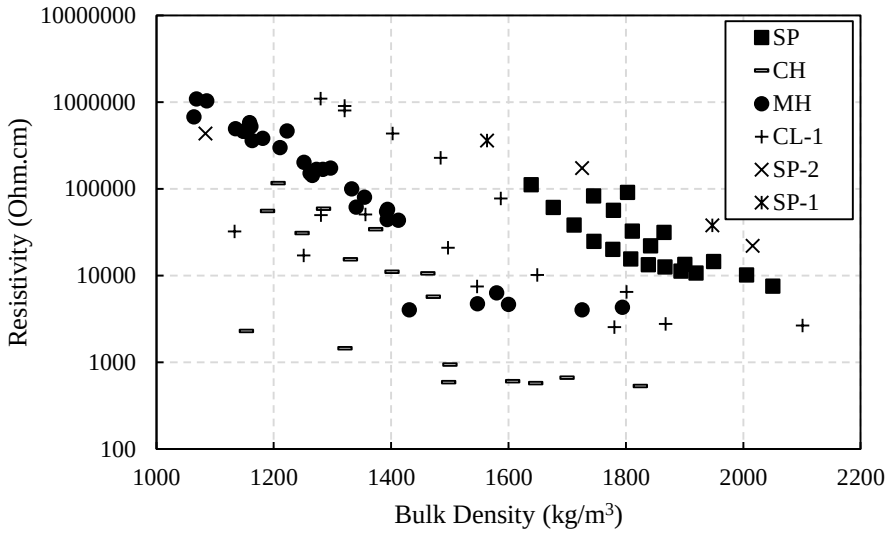


Figure 30 – Results of two different types of sands from Arkansas (SP-1 and SP-2) plotted along with other major soil types

### 4.5 Additional Considerations

As discussed, the only ML that could be sourced as a benchmark sample was a processed kaolin clay. This soil classified as ML with a liquid limit of 34 and a plasticity index of 6. The results are presented in Figure 31 along with the results of the CH benchmark soil. As shown in the figure, the processed kaolin clay is indistinguishable from the CH soil and appears very differently from the unprocessed kaolin (MH). Further analysis of the kaolin clays through Energy-dispersive X-ray spectroscopy (EDX) revealed that the unprocessed Kaolin was a sodium-potassium ($Na^+$-$K^+$) kaolinite with 25% sodium and 11% potassium cations while the processed Kaolin was a sodium-calcium ($Na^+$-$Ca^{2+}$) kaolin with 33% sodium and 24% calcium. Therefore, despite the similar name, mineralogicaly speaking they are different soils with different cation exchange capacities (CEC). The presence of $Ca^{2+}$ cations in the processed kaolin likely causes the lower resistivity compared to the unprocessed kaolin. This finding reveals the importance of mineralogy in the measured resistivity of soils.

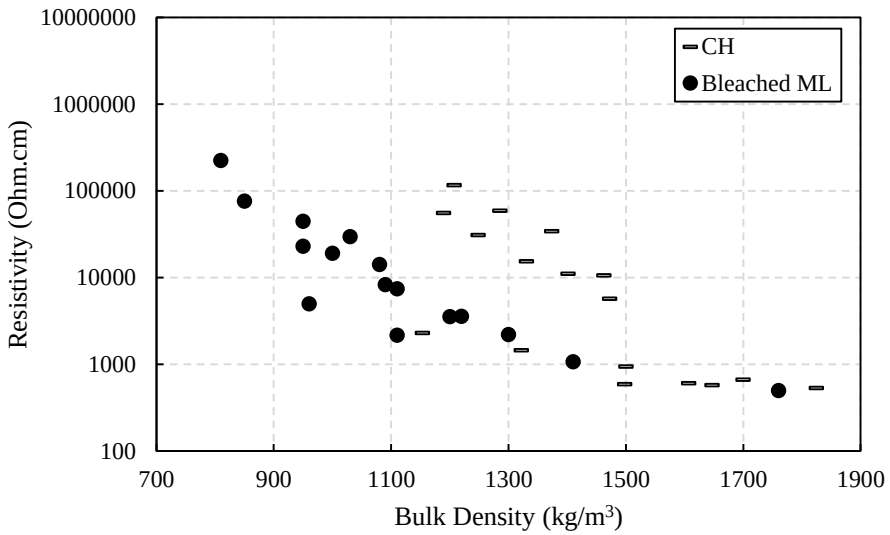


Figure 31 - Resistivity of processed Kaolin clay in comparison with the CH soil type

## 4.6 Application

After gaining an understanding of the effect of various parameters on the resistivity of soils, this knowledge needs to be applied to the interpretation of resistivity data collected in the field. As seen in Figure 22 and Table 4, when the soil is below the water table, the measured resistivity is not sensitive to the density, water content and water quality. Therefore, if the location of the water table is known, the soil type for soils below the water table can be distinguished. Under this condition, a chart in the format of Figure 32 shall be used to predict soil type. As can be seen, most of the soil types tested can be easily distinguished based on their resistivities under saturated conditions.

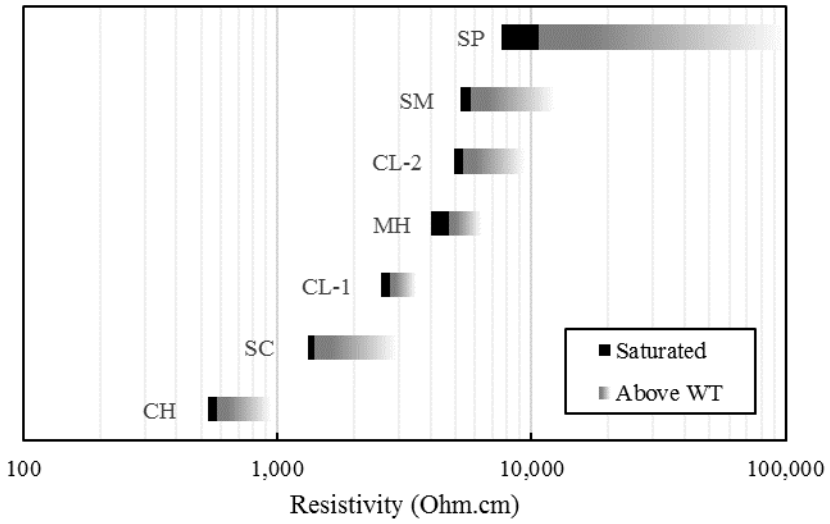


Figure 32 - Expected resistivity for different soil types above water table (up to approximately 25m)

Distinguishing soil types above the water table is more challenging due to the broader range of water content and the increased effect of density on resistivity. Moreover, matric suction will cause water to rise above the water table at different heights depending on the soil type and particle sizes. However, several steps could be taken to simplify this part as well. For example, it is known that water does not rise in sands more than one meter (for typical gradations in nature), while clays may remain at water contents close to saturation for tens of meters above the water table (Fredlund et al., 2012). It should be noted that other phenomenon such as rain, flooding, extreme heat or humidity could alter the moisture content of these soils and should be carefully considered when planning a resistivity survey. Therefore, under normal conditions and having known the depth of water table, sands should show the whole range of their resistivity in the first meter above the water table ($10^4$-$10^5$ ohm.cm); any sand more than one meter above the water table is likely to have a resistivity in the order of $10^5$ ohm.cm. However, clays hold water contents close to saturation tens of meters above the water table and the actual height depends on

their soil water characteristics curve (SWCC). As can be seen in the generic SWCC plots presented in Figure 33, clays can be assumed saturated up to 10 meters above the water table (98 kPa suction) and the suction decreases gradually above 10 meters although they still maintain a relatively high water content up to 100 meters (980 kPa suction) above the water table. As water tables deeper than 25 meters are hardly encountered unless it is extreme desert conditions, the results in Figure 33 were plotted for the depth of 25 meters to make it more applicable to typical field studies conducted for geotechnical purposes.

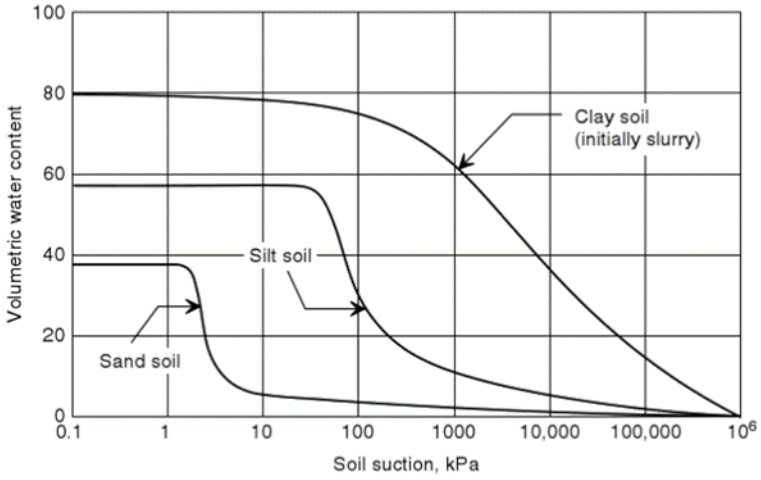


Figure 33 - Comparative desorption SWCCs for sand, silt, and clay soils (Fredlund et al., 2012)

Therefore, it is safe to use charts similar to Figure 32 to discern different soil types up to 25 meters above the water table. While most of the tested soil types do not have any overlap in their range of resistivities, some such as CL-2, MH and SM do. A closer look at the composition of these soils (Table 3) shows that they are all composed of Kaolinite. Therefore, resistivity is consistent for similar minerals and can perhaps give information about the mineral present.

## 4.7 Conclusions and Future Work

This thesis summarizes an investigation on the relationships between geotechnical parameters such as saturation, volumetric water content, dry density, bulk density and soil classification parameters with laboratory-based electrical resistivity measurements in order to determine soil type. Benchmark samples made from combinations of commercially available soils were tested at various water contents and densities to create plots that could be used to predict soil type for natural samples. Several validation studies were also conducted using natural soils to examine the effectiveness of the developed charts.

The results indicate that there is clear correlation between these parameters and the resistivity of soil. An increase in either of those parameters is associated with a decrease in electrical resistivity. However, the effect of these parameters is not linear and is affected by other parameters. For example, the resistivity values were found to be highly dependent on the degree of saturation up to approximately 60%, at which point increasing saturation did not result in significantly different resistivity values. When the soil is close to saturation, the effect of density or water quality on resistivity diminishes significantly which makes the task of identifying soil type easier. Among the parameters investigated, it was observed that bulk density in conjunction with electrical resistivity can offer the best estimate of soil type.

For most field cases, bulk density is not easily obtained and although this information was available for the lab samples, it would not likely be available for a true non-destructive field study. Because the ultimate goal of the work was to develop charts that could be used to estimate soil type for field retrieved data, another approach to interpret resistivity surveys based on the obtained dataset was proposed in the “Application” section. This approach was based on

the idea that the location of the water table was either known or could be determined in the field. The results plotted in Figure 27 shows that soils below the water table can easily be distinguished based on their resistivity alone. However, uncertainty in interpretation increases above the water table as the soils can have a broader range of electrical resistivity depending on water content and density and this uncertainty increases as the depth to the water table increases. When interpreting the resistivity results above the water table, an estimate of water content is necessary which could be affected by the climate condition, matric suction and the SWCC.

While they were not perfect predictions in all cases, some of the verification studies show that resistivity may be significantly affected by the mineral composition of the soil. For example, the last case studied in section 4.5 shows that a processed sodium Kaolinite, classifying as ML, may appear the same way as a CH on a bulk density-resistivity plot. This finding, while interesting, needs to be further investigated. Only a limited number of natural soil samples were investigated and it is recommended that a larger number of data points from natural samples be added to the curves in the future. The results also further indicate the need for building a database for different soil types found across the globe. A database of soil properties and corresponding resistivity values would allow for statistical analysis of the data and for a more precise prediction model to be generated. The next phase of the work should also include a comparison with field resistivity profiles and the resistivity values obtained in the laboratory for samples retrieved within the profile. This type of work would provide an additional blind study which could prove very useful in determining the effectiveness of the charts developed as a part of this research.

## References


AASHTO. (2012). Standard T 288-12. Standard method of test for determining minimum laboratory soil resistivity. Washington, DC: American Association of State Highway and Transportation Officials.

Allaud, L., & Martin, M. (1977). Schlumberger: The history of a technique Wiley.

American Society of Civil Engineers (ASCE). (2007). The New Orleans hurricane protection system: What went wrong and why

Archie, G. E. (1942). The electrical resistivity log as an aid in determining some reservoir characteristics, 146-154.

American Society of Civil Engineers (ASCE). (2013). Report card for America's infrastructure American Society of Civil Engineers.

American Society of Civil Engineers (ASCE). (2017). 2017 Infrastructure report card: Levees. American Society of Civil Engineers.

ASTM D2487-11 (2011). Standard practice for classification of soils for engineering purposes (unified soil classification system). ASTM International.

ASTM G57-06 (2012). Standard test method for field measurement of soil resistivity using the Wenner four-electrode method. ASTM International.

Besson, A., Cousin, I., Samouëlian, A., Boizard, H., & Richard, G. (2004). Structural heterogeneity of the soil tilled layer as characterized by 2D electrical resistivity surveying. Soil and Tillage Research, 79(2), 239-249.

Briaud, J. L., Chen, H., Govindasamy, A. V., & Storesund, R. (2008). Levee erosion by overtopping in New Orleans during the Katrina hurricane. Journal of Geotechnical and Geoenvironmental Engineering, 134(5), 618-632.

Briaud J.-L., Ting F., Chen H.C., Cao Y., Han S.-W., Kwak K., (2001). Erosion Function Apparatus for Scour Rate Predictions, Journal of Geotechnical and Geoenvironmental Engineering, 127(2), 105-113.

Chlaib, H. (2014). Geophysical applications for levee assessment. Scholars' Press.

Dahlin, T. (2001). The development of DC resistivity imaging techniques. Computers & Geosciences, 27(9), 1019-1029.

Davis, J. L., & Annan, A. P. (1989). Ground-penetrating radar for high-resolution mapping of soil and rock stratigraphy. Geophysical Prospecting, 37(5), 531-551.

Dunbar, J., Stefanov, J., Bishop, M., Peyman-Dove, L., Llopis, J., Murphy, W., et al. (2003). An integrated approach for assessment of levees in the lower Rio Grande valley. Symposium on the application of geophysics to engineering and environmental problems 2003 (pp. 350-362) Environment and Engineering Geophysical Society.

Ellis, H., Groves, C., & Fischer, G. (2008). Rapid levee assessment for reliability and risk analysis. Geo-Congress: The Challenge of Sustainability in the Geoenvironment, New Orleans, LA. pp. 170-177.

Everett, M. E. (2013). Near-surface applied geophysics Cambridge University Press.

Florides, G., & Kalogirou, S. (2005). Annual ground temperature measurements at various depths. 8th REHVA World Congress, Clima, Lausanne.

Fredlund, D. G., Rahardjo, H., & Fredlund, M. D. (2012). Unsaturated soil mechanics in engineering practice Wiley.

Hayashi, K., & Konishi, C. (2010). Joint use of a surface-wave method and a resistivity method for safety assessment of levee systems. 2010 Geo-Congress: Advances in Analysis, Modeling & Design, West Palm Beach, FL. , Geo-Congress: Advances in Analysis, Modeling & Design. pp. 1340-1349.

Hayashi, K., Inazaki, T., Kitao, K., & Kita, T. Statistical soil type estimation using cross-plots of S-wave velocity and resistivity in japanese levees

Inazaki, T., & Sakamoto, T. (2005). Geotechnical characterization of levee by integrated geophysical surveying. Proceedings of the International Symposium on Dam Safety and Detection of Hidden Troubles of Dams and Dikes,

Herman, R. (2001). An introduction to electrical resistivity in geophysics. American Journal of Physics, 69(9), 943-952.

Jean-Louis Briaud. (2008). Case histories in soil and rock erosion: Woodrow wilson bridge, brazos river meander, normandy cliffs, and new orleans levees. Journal of Geotechnical and Geoenvironmental Engineering, 134(10), 1425-1447.

Kaufman, A. A., & Hoekstra, P. (2001). Electromagnetic soundings Elsevier Science B.V.

Keller, G. V., & Frischknecht, F. C. (1966). Electrical methods in geophysical prospecting Pergamon Press.

Kita, T., Inazaki, T., & Hayashi, K. (2013). 2-dimensional linear array microtremor survey techniques for earthen levee investigations. Proceedings of the 11th SEGJ international symposium, yokohama, japan, 18-21 november 2013 (pp. 214-217) Society of Exploration Geophysicists of Japan.

Kusuda, T., & Achenbach, P. R. (1965). Earth temperature and thermal diffusivity at selected stations in the united states No. NBS-8972). National Bureau of Standards Gaithersburg MD: DTIC.

Lane, J., Ivanov, J., Day?Lewis, F., Clemens, D., Patev, R., & Miller, R. (2008). Levee evaluation using MASW: Preliminary findings from the citrus lakefront levee, new orleans, louisiana. Symposium on the application of geophysics to engineering and environmental problems 2008 (pp. 703-712) Environment and Engineering Geophysical Society.

Llopis, J., & Simms, J. (2007). Geophysical surveys for assessing levee foundation conditions, feather river levees, marysville, CA. Symposium on the application of geophysics to engineering and environmental problems 2007 (pp. 82-89) Environment and Engineering Geophysical Society.

Loke, M. (1999). Electrical imaging surveys for environmental and engineering studies: A practical guide to 2-D and 3-D surveys.

McKenna, J., Dunbar, J., Wakeley, L., & Smullen, S. (2006). Near surface geophysical methods to assess levee integrity and potential failure. Symposium on the application of geophysics to engineering and environmental problems 2006 (pp. 320-326) Environment and Engineering Geophysical Society.

McNeill, J. D. (1980). Electromagnetic terrain conductivity measurement at low induction numbers. Mississauga, Ontario, Canada: Geonics Ltd.

Mihalakakou, G., Santamouris, M., Lewis, J., & Asimakopoulos, D. (1997). On the application of the energy balance equation to predict ground temperature profiles. Solar Energy, 60(3-4), 181-190.

Miller, R., & Ivanov, J. (2005). Seismic tests on IBWC levees: Weslaco, Texas No. Open-file Report No. 2005-56). Lawrence, Kansas: Kansas Geological Survey.

NOAA. (2017). What is LIDAR?., 2017, from http://oceanservice.noaa.gov/facts/lidar.html

Palacky, G. (1988). 3. resistivity characteristics of geologic targets. Electromagnetic methods in applied geophysics (pp. 52-129) Society of Exploration Geophysicists.

Palaseanu-Lovejoy, Monica, Cindy A. Thatcher, and John A. Barras. "Levee Crest Elevation Profiles Derived from Airborne Lidar-Based High Resolution Digital Elevation Models in South Louisiana." ISPRS Journal of Photogrammetry and Remote Sensing 91 (2014): 114-26.

Piegari, E., & Maio, R. D. (2013). Estimating soil suction from electrical resistivity. Natural Hazards and Earth System Sciences, 13(9), 2369-2379.

Rutherford, C., Pinter, N., Gamez, J., Harder, L., Lobbestael, A., Musgrove, M., et al. (2016). Preliminary observations of levee performance and damage following the 2015-16 Midwest floods in Missouri and Illinois, USA No. GEER-045) Geotechnical Extreme Events Reconnaissance (GEER).

Sasaki, Y., Tamura, K., Yamamoto, M., & Ohbayashi, J. (1995). Soil improvement work for river embankment damage by 1993 Kushiro Oki earthquake. The First International Conference on Earthquake Geotechnical Engineering, Tokyo, Japan. , 1. pp. 43-48.

Seladji, S., Cosenza, P., Tabbagh, A., Ranger, J., & Richard, G. (2010). The effect of compaction on soil electrical resistivity: A laboratory investigation. European Journal of Soil Science, 61(6), 1043-1055.

Sharma, P. V. (1997). Environmental and engineering geophysics Cambridge University Press.

Stokoe, K. H., Roesset, J., Bierschwale, J., & Aouad, M. (1988). Liquefaction potential of sands from shear wave velocity. Proceedings, 9nd World Conference on Earthquake, , 13. pp. 213-218.

The Federal Emergency Management Agency (FEMA), Department of Homeland Security. (2006). Emergency Management and Assistance, Title 44, V. 1.

US Army Corps of Engineers (USACE). National levee database. https://nld.usace.army.mil/egis/f?p=471:1:2106562061116

Van Genuchten, M. T. (1980). A closed-form equation for predicting the hydraulic conductivity of unsaturated soils. Soil Science Society of America Journal, 44(5), 892-898.

Vrjiling, J. K. (2003). Probabilistic design and maintenance of water defense systems. Risk-Based Maintenance of Civil Structures, 8th Series Workshop, Delft, Netherlands.